

Palaeoecological studies on the development of the world's southernmost palm-swamp peatland ecosystem in Kosi Bay, South Africa

Marvin Gabriel ^{a,*}, Jemma Finch ^{b,c}, Klaus-Holger Knorr ^d, Amanda Khuzwayo ^b, Graeme T. Swindles ^{e,f}, Mariusz Gałka ^g

^a Nature and Biodiversity Conservation Union, Team Ecological Restoration, Charitéstraße 3, 10117 Berlin, Germany

^b School of Agricultural, Earth and Environmental Sciences, University of KwaZulu-Natal, Private Bag X01, Scottsville 3200, South Africa

^c South African Environmental Observation Network (SAEON), Grasslands, Forests, Wetlands Node, Montrose, 3201, South Africa

^d Institute for Landscape Ecology, Ecohydrology and Biogeochemistry Group, Heisenbergstr. 2, University of Münster, 48149 Münster, Germany

^e Geography, Department of Geography, School of Natural and Built Environment, Queen's University Belfast, UK

^f Ottawa-Carleton Geoscience Centre and Department of Earth Sciences, Carleton University, Ottawa, Canada

^g University of Łódź, Faculty of Biology and Environmental Protection, Department of Biogeography, Paleogeology and Nature Conservation, Banacha 1/3, 90-237 Łódź, Poland

ARTICLE INFO

Keywords:

Tropical wetland
Histosol
Raphia
Macrofossil analysis
Carbon sequestration
Peat qualities

ABSTRACT

Palm-swamps are known as peat forming environments from several tropical regions. The southernmost peat forming palm-swamps lie in Kosi Bay, at the South African East Coast (27° southern latitude), consisting of scattered homogeneous stands of *Raphia australis* Oberm. and Strey. It is the only *Raphia* species endemic to southern Africa and red listed. This study investigates the genesis of a *R. australis* palm-swamp peatland at Kosi Bay. Environmental reconstruction based on plant macrofossils, pollen, elemental composition and peat qualities, supported by AMS radiocarbon dating unveiled that: i) a shallow peat layer (ca. 55 cm) has accumulated since about 1000 CE under a regionally warm and wet climate, with the first peat forming vegetation community composed of sedges, including *Pycreus polystachyos* and *Cyperus* sp. Around 1370 CE a shift to swamp forest occurred. *R. australis* became established around 1550 CE, following a fire and becoming dominant around 1900 CE; ii) peat accumulation occurred since then at a low rate of 0.038 mm yr^{-1} ($19 \text{ g m}^{-2} \text{ yr}^{-1}$), which is especially low for top soil peat layers, yet indicates rather steady hydrologic conditions on the floodplain with currently low peat accumulation potential. *Raphia* peat is highly decomposed, with high contents of aromatics, aliphatics, and also of amids. Peat forming parts are the roots, leaves become decomposed in the surface layer; iii) the ecological conditions (eutrophic: C/N 14–20; slightly acid: pH 5–6) resemble rather Amazonian *Mauritia flexuosa* palm-swamps peatlands than *Raphia* peatlands of the Congo Basin.

Editor: Dr. Howard Falcon-Lang.

1. Introduction

Natural intact peatlands sequester CO₂ and are therefore of great importance for mitigating climate change. It is estimated that approximately 600 Gt of carbon are stored in peatlands around the globe (Yu et al., 2010). By the removal of atmospheric CO₂, peatlands have contributed a net cooling effect on global climate of about 0.6 °C over

the past 10,000 years (Kirpotin et al., 2021). Drained peatlands, on the contrary, contribute to global warming, when formerly sequestered carbon becomes oxidised and liberated as CO₂ back to the atmosphere (Joosten et al., 2016). Moreover, intact peatlands are of vital importance for biodiversity, representing habitats for specialised aquatic and semi-aquatic species (Minayeva and Sirin, 2012). Given the global climate and biodiversity crises, peatlands have received much scientific attention in recent decades (van Bellen and Larivière, 2020).

In contrast to the other world regions, where peatlands are already

Abbreviations: HI, Humification Index; MCP, Maputaland Coastal Plain; AMS, Accelerator mass spectrometry; FTIR, Fourier-transform infrared spectroscopy; XRF, X-ray fluorescence; IUCN, International Union for Conservation of Nature.

* Corresponding author.

E-mail addresses: marvin.gabriel@posteo.de (M. Gabriel), Finchj@ukzn.ac.za (J. Finch), kh.knorr@uni-muenster.de (K.-H. Knorr), g.swindles@qub.ac.uk (G.T. Swindles), mariusz.galka@biol.uni.lodz.pl (M. Gałka).

<https://doi.org/10.1016/j.palaeo.2025.113217>

Received 2 July 2025; Received in revised form 18 August 2025; Accepted 18 August 2025

Available online 21 August 2025

0031-0182/© 2025 Elsevier B.V. All rights are reserved, including those for text and data mining, AI training, and similar technologies.

well studied (especially the northern temperate and boreal zones and for tropical peatlands the Malayan Archipelago), peatlands on the African continent remain relatively understudied (van Bellen and Larivière, 2020). One type of peatland, which is common in the African tropical regions are palm-swamps (Bord na Móna, 1985; Dargie et al., 2017; Elshehawi et al., 2019a). A special role of peat accumulation through palms comes to the genus *Raphia*. It includes in total 21 species and, with the exception of one species (*R. taedigera*), is a solely African genus (Helmstetter et al., 2020). In several countries of tropical Africa, including Guinea and Liberia, *Raphia* (species unspecified) is assigned as a peat forming vegetation (Bord na Móna, 1985). Currently, much attention is given to peatlands in the Congo Basin, where *Raphia* is the most important genus in palm-dominated swamp forests, especially the species *R. laurentii* (Dargie et al., 2017; Bocko et al., 2023; Hawthorne et al., 2023). All 21 *Raphia* species are native to tropical Africa, with *R. taedigera* co-occurring in Central America (Urquhart, 1999a). *Raphia taedigera* is a coloniser, initiating peat formation in coastal freshwater swamps (Toxler, 2007), known from Costa Rica (Obando and Malvassi, 1993; Mitsch et al., 2010), Nicaragua (Urquhart, 1999b) and Panama (Hoyos-Santillan et al., 2016; Phillips and Bustin, 1996; Toxler, 2007).

In the southern part of Africa, the only naturally occurring *Raphia* species is *R. australis* (Mattson and Uken, 2007). It is associated with freshwater swamp forest, although it tends to occur in the drier parts of these habitats (Grobler et al., 2004). The species is, however, adapted to water saturated soils and its roots are pneumatophores (Obermeyer and Strey, 1969). It is endemic to South Africa and southern Mozambique, where it is restricted to several areas with mostly homogenous stands (Matimele et al., 2016; Obermeyer and Strey, 1969). *R. australis* has a monocarpic reproduction, i.e. all mature individuals in a homogenous stand flower simultaneously just once in their lifetime, usually at an age of about 18–24 years (Mattson and Uken, 2007; Grobler, 2009).

According to the IUCN red list, *R. australis* stands are ranked as ‘vulnerable’, with an estimated population size of approximately 6000 individuals remaining in their natural habitat, with decreasing numbers throughout their range (Matimele et al., 2016). At present, the remaining natural stands of *R. australis* are restricted to four fragmented subpopulations along the East Coast of southern Africa. The northernmost subpopulation is situated close to Chidenguele (24°55' S, 34°11' E; Mozambique) and the southernmost at Kosi Bay (27°02' S, 32°49' E; South Africa) (Matimele et al., 2016). The populations in Mozambique are especially threatened, due to habitat transformation linked to expanded rice farming, subsistence agriculture, and housing construction (Matimele et al., 2016). Local community uses for the species have so far not threatened *R. australis* populations, as mostly the midribs of fallen leaves are used (Grobler et al., 2004). Traditionally, the up to 10 m long leaves are used as construction material for huts and market stands, as well as small boats and rafts (Mattson and Uken, 2007; Obermeyer and Strey, 1969). Considering the sustainability of the harvesting practice, Sliva et al. (2004) even suggest propagating *Raphia* palms to counteract the loss of swamp forest areas.

The extent and characteristics of *R. australis* swamp forest in South Africa have been examined by Smuts (1992). He indicated *R. australis* swamp forests as a peat forming vegetation at the borders of the Siyadla River and the shores of Lake Amanzimyama (meaning *black water* in the local language isiZulu, referring to dissolved/particulate organic matter originating from the peatlands in the watershed). He notes that peat is usually found in sapric (highly decomposed) conditions. It is known that *R. australis* peat contains considerably lower organic matter content (ca. 62 %) than peat types more frequent in the region, like sedge peat (75–93 %) or woody swamp forest peat (82–94 %) (Gabriel et al., 2017b; Gabriel et al., 2018). Nevertheless, no previous research has investigated the genesis of a *R. australis* covered peatland and studied the peat characteristics in further detail.

The objectives of this study are therefore 1) to unveil the genesis of a peatland currently dominated by *R. australis*; 2) to explore typical peat characteristics 3) to investigate carbon accumulation dynamics; and 4)

to determine the ecological conditions of the *R. australis* habitat.

2. Materials and methods

2.1. Study area

The study area is the southernmost population of *R. australis*, situated in Kosi Bay, South Africa (Fig. 1 a-d). The area is characterised by a system of four lakes, connected by small channels, followed by tidal flats and an outflow to the Indian Ocean, the so-called Kosi Mouth (Begg, 1980). Kosi Bay lies in the northern part of the Maputaland Coastal Plain (MCP), whose undulating dune surface consists of unconsolidated wind re-distributed Holocene sands (Botha and Porat, 2007; Maud, 1980).

The climate is subtropical-tropical, with an annual precipitation of about 840 mm and monthly average temperatures between 26 °C in February and 19 °C in June (Climate-data.org, accessed 21.10.2024). About 60 % of the precipitation occurs in the austral summer from November to March and the annual evapotranspiration reaches up to 2200 mm (Water Research Commission, 2012). Therefore, groundwater fed minerotrophic peatlands in interdune depressions and valley-bottoms are common landscape features on the MCP, which hosts about two thirds of South Africa's peatland area (Grundling et al., 1998). Peatlands, which are defined by Joosten and Clarke (2002) as areas with “sedentarily accumulated material of at least 30% (dry mass) of dead organic material”, are on the MCP typically vegetated with grasses (mainly Cyperaceae) or swamp forest trees (mainly *Syzygium cordatum*, *Voacanga thouarsii*, *Ficus trichopoda*). *R. australis* is very rare and its population is situated on the western shores of Lake Amanzimyama, and on the flood plain of the Siyadla River, close to its mouth with the lake (Fig. 1 d). The scattered *R. australis* stands there cover an area of about 70 ha. A homogenous stand of about 3 ha with mature palms and underlying peat was selected for the current study. The site (27°02'23"S; 32°49'05"E) lies on the flood plain, at 7 m a.s.l. and at a distance of 4 km from the Ocean. The tree stratum consisted of more than 90 % *R. australis*, with a few small individuals of *Ficus trichopoda* and *Syzygium cordatum*. In the herbal stratum, only the fern *Stenochlaena tenuifolia* was encountered, covering about 10 % of the ground.

2.2. Field sampling, soil profile description, determination of bulk density, and pH

The vertical extent of the peat layer in the selected *Raphia* stand (see Fig. 1d) was tested at several locations using a Russian Peat Corer. The point with the thickest peat layer was selected as a sampling site for detailed palaeoecological analysis. A profile pit was dug with a spade, for the first 30 cm below the surface. As water ran into it, the lower part of the profile was explored with a peat core. The soil description was done using the German Soil Mapping Manual KA5 (Ad-hoc-AG Boden, 2005) and later translated into the terminology of the World Reference Base for Soil Resources “WRB” (FAO, 2015). A half-cylindrical sample core was extracted, with the Russian Peat Corer, 49 cm long and 5.2 cm wide. The core was packed in a plastic tube, wrapped in plastic foil and refrigerated at 5 °C until further processing. The tip of the Russian Peat Corer was unable to penetrate the underlying sand layer; however, an Edelmann Auger was used to establish a total peat depth of 55 cm. A triplicate of volumetric sample rings was taken for each horizon and dried for 48 h at 105 °C (DIN EN 15934: 2012-11, n.d.). Values of pH were determined for each horizon with a field electrode (Eutech CyberScan PC 650).

2.3. Peat core chronology

The chronology of the peat sequence was determined by accelerator mass spectrometry (AMS) radiocarbon dating of three selected samples of plant macrofossils (Table 1). Radiocarbon dating was undertaken at the Poznań Radiocarbon Laboratory. The calibration of the radiocarbon

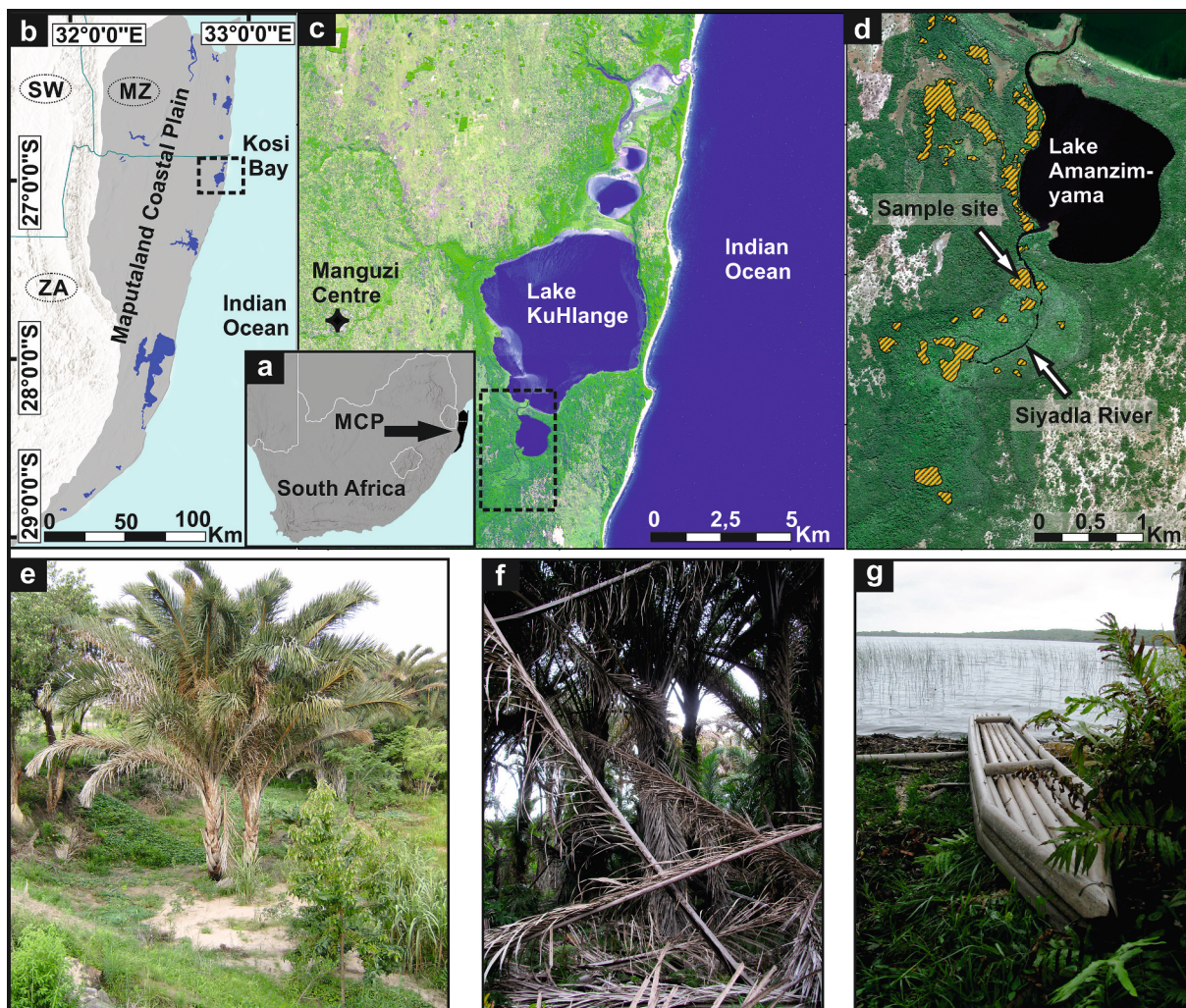


Fig. 1. a) Position of the Maputaland Coastal Plain (MCP) in southern Africa; b) Close up on the MCP with Kosi Bay in the dashed box; c) Satellite image (SPOT 5, 2010) of the Kosi Bay Lake System, the area around Lake Amanzimyama and the Siyadla River in the dashed box; d) Satellite image of the floodplain of the Siyadla River and Lake Amanzimyama with adjacent areas. Dashed orange areas indicate homogenous *R. australis* stands; e) Juvenile *R. australis* palm (credits for the photo: Naret Guerrero Moreno); f) Sample site, *R. australis* swamp forest with fallen leaves; g) raft constructed from the midribs of *R. australis* leaves.

Table 1
Dated material, ^{14}C date, calibrated age (AD), vertical accumulation rate.

Site/Depth (cm)	Material	Nr. Lab.	^{14}C date	Cal Age (95,4 %)	Acc. rate (cm yr^{-1})
RAP 5–6	Leaf fragment	Poz-106,615	$110 \pm 0.33 \text{ pMC}$	1892–1923 CE	0.038
RAP 23–25	Charred wood	Poz-106,577	$595 \pm 30 \text{ BP}$	1321–1436 CE	0.039
RAP 48–49	Charcoal	Poz-106,543	$960 \pm 30 \text{ BP}$	1031–1207 CE	0.075

dates and the construction of the age-depth model was performed with OxCal 4.4 (Bronk-Ramsey, 2009) and calibrated using the SHCal20 atmospheric curve (Hogg et al., 2020) applying a P_Sequence function with a k parameter of 1 cm^{-1} and 1-cm resolution.

2.4. Palaeobotanical analysis

High-resolution (1-cm peat slices) plant macrofossil analysis was used to reconstruct local plant succession. The contiguous samples had a volume of approximately 5 cm^3 . The samples were washed and sieved under $30\text{--}35^\circ\text{C}$ warm water over 0.20 mesh screens. The entire samples were analysed with a stereoscopic microscope. Individual plant macrofossils (seeds and fruits) were identified with the help of appropriate keys (Cook, 2004; Gordon-Gray, 1995) and a self-gathered collection of wetland plant seeds (Gabriel, 2019). The content of living and dead

radicells was estimated, as well as *R. australis* leaf fragments.

The plant macrofossils have been summarised in the diagram in absolute numbers. Macroscopic charcoal fragments ($< 1 \text{ mm}$ and $> 1 \text{ mm}$) were also counted during plant macrofossil analysis and their presence provides information on past local fire occurrence (Mooney and Tinner, 2011).

The peat core was further subsampled at a 2 cm resolution for fossil pollen analysis, yielding 25 subsamples (1 cm^3 each). Subsamples were processed using standard palynological methods of HCl, NaOH and HF digestion (Faegri and Iverson, 1989) and mounted using semi-permanent Aquatex gel. Identification was achieved using a Leica DM750 microscope at magnifications of $400 \times$ and $1000 \times$. A minimum count of 400 grains was achieved in all but two samples, with an average pollen count of >600 grains. Pollen identification was facilitated using the reference collection in the University of KwaZulu-Natal

Palaeoecology Laboratory, and published works (e.g., Scott, 1982). Pollen reference slides for *R. australis* were created using a flowering specimen derived from the University of KwaZulu-Natal Botanical Garden in Pietermaritzburg. Pollen taxa were arranged according to ecological groupings as follows: herbs and shrubs, grasses, aquatics, swamp forest and coastal forest (Table S1). Due to limited taxonomic resolution of pollen identifications and broad ecological preferences of some taxa, these ecological groupings are not intended to serve as discrete units, but rather to assist interpretation and data description. Stratigraphic macrofossil and pollen diagrams were plotted using C2 (Juggins, 2007).

Stratigraphically Constrained Incremental Sum of Squares (CONISS) cluster technique (Grimm, 1987) within Psimpoll (Bennett, 2009) was used to define boundaries between different episodes in the peatland's genesis, by analysing percentage values of macrofossils (fruits, seeds) and pollen (Supplementary Fig. S1).

2.5. Testate amoebae

A sample of the dimension 1 cm³ was extracted every second vertical centimetre for testate amoebae analysis. Testate amoebae were extracted from each sample following Booth et al. (2010).

2.6. Elemental analyses

Bulk samples of 4x1x1 cm were extracted from 12 consecutive intervals, covering 0–48 cm of the sample core, for analyses of the substrates' chemical composition. To this end, bulk samples were freeze dried (Alpha 1–4 LD plus, Christ, Osterode, Germany) and subsequently milled to powder in a ball mill, using tungsten carbide grinding tools (MM400, Retsch, Haan, Germany). Peat total carbon and nitrogen was determined by weighing 3–4 mg of sample into tin capsules and subsequent catalytical combustion using an elemental analyser (EA3000, Eurovector/HEKAttech, Wegberg, Germany). Further element concentrations (Al, Ca, Cl, Fe, K, Mg, Mn, Na, P, S, Si, Ti, Zn) were determined by means of non-destructive, wavelength-dispersive X-Ray fluorescence spectroscopy (WD-XRF; ZSX Primus II, Rigaku, Tokyo, Japan), calibrated for peat and plant material using certified reference materials. To do so, 500 mg of sample were pressed to a 13 mm pellet, using a pellet die and a hydraulic press (Specac, Orpington, UK). The pellet was subsequently analysed by WD-XRF. Bulk elemental contents and elemental ratios were plotted over depth.

2.7. Peat quality

Material from the same sample as for the X-ray fluorescence spectroscopy served for analysis of peat chemical quality by Fourier transformed Infrared spectroscopy (FTIR), determining a humification index following Broder et al. (2012). This humification index relates the spectral absorption at a peak indicative of aromatics and lignin (wavenumber ~1630 cm⁻¹) to the absorption indicative of carbohydrates (wavenumber ~1090 cm⁻¹) (Broder et al., 2012). Moreover, we calculated putative contents of holocellulose and Klason lignin, as derived from FTIR spectra and following Hodgkins et al. (2018). This approach is not without caveats, in particular potential overlap of bands used to predict Klason Lignin with N—H bending of proteins (Teickner and Knorr, 2022). Spectra were recorded on an FTIR spectrometer (Cary 660, Agilent, Santa Clara, USA) in the wavenumber range from 600 to 4000 cm⁻¹. An amount of 2 mg of sample was mixed with 200 mg of KBr (FTIR grade, Sigma Aldrich, St. Louis, MO, USA) and pressed to a 13 mm pellet using similar equipment as described above for WD-XRF. For each sample 32 spectral scans were averaged, spectra were background corrected and normalized. Spectral processing and calculation of indices was done using R 4.0.3 (R Core Team, 2020) and available toolboxes ir (0.0.0.9000) (Teickner, 2020) and irpeat (0.0.0.9000) (Teickner and Hodgkins, 2020).

2.8. Peat accumulation rates

The vertical peat accumulation rate (VAR) was calculated for the substrate corresponding to each dated depth according (eq. 1).

$$VAR = \frac{E}{Age_{ul} - Age_{ll}} \quad (1)$$

E = vertical extent of a layer; Age_{ll} = age (from age-depth model) of lower layer boundary; Age_{ul} = age (from age-depth model) of upper layer boundary.

The carbon accumulation rate (CAR), which gives the amount of carbon per m² for a determined time interval, was calculated for each substrate according (eq. 2).

$$CAR = \frac{E \times BD \times C \times A}{Age_{ul} - Age_{ll}} \quad (2)$$

BD = bulk density of the dry mass [g/cm³]; C = carbon content [g_{carbon}/g_{soil}]; A = 10,000 (factor to convert unit from cm² to m²).

The long-term apparent rate of carbon accumulation (LORCA), referring to the average amount of carbon, annually stored in the peatland as a whole (Clymo et al., 1998), is calculated according eq. (3).

$$LORCA = \frac{M_T}{T} \quad (3)$$

M_T = cumulative dry mass of carbon at time [T] of each layer, as calculated according eq. (4)

$$M_T = \sum_i^n (E_i \times BD_i \times C_i \times 10000) \quad (4)$$

i = index for layer.

3. Results

3.1. Soil profile

On top of the soil was a dense litter layer, mainly formed by fragments of decomposing *R. australis* leaves (Fig. 2). Underneath, from 0 to 5 cm of depth, was a dense felt of interwoven living rootlets in a matrix of hemic peat. From 5 to 15 cm depth, many living rootlets were found, which gradually decreased in abundance until 25 cm. The matrix consisted of sapric peat. At 25 cm there was an abrupt change to hemic peat below that depth, with fewer living rootlets in the soil matrix, but still moderately pervaded by both living and dead roots >5 mm. The degree of decomposition steadily decreased to fibric peat before encountering an abrupt change to middle grained sand at 55 cm depth. This transition from peat to the mineral underground was explored with an Edelman auger, so no soil sample material was taken below 49 cm.

3.2. Radiocarbon dating, age depth model and peat accumulation rates

Radiocarbon dating revealed that the peat layer at a depth of 48–49 cm had accumulated between 1030 CE and 1200 CE (Table 1), 1060 CE according to the age depth model. Two further radiocarbon dates and the age-depth model (Fig. 3) suggest that there was no hiatus in peat accumulation. Two different accumulation characteristics can be seen (Fig. 3). The vertical peat accumulation rate for 48–25 cm was 0.075 cm yr⁻¹, for 25–6 cm it was 0.039 cm yr⁻¹ and from 6 to 0 cm 0.038 cm yr⁻¹. The initiation of the peatland from 55 cm depth, likely took place around 970 CE under the given vertical peat accumulation rate.

3.3. Palaeoenvironmental analysis

Overall fossil pollen preservation was excellent with a total of 48 pollen taxa recorded (Supplementary Table S1), and a high proportion of arboreal taxa present (Fig. 5). A full diagram including rare taxa present

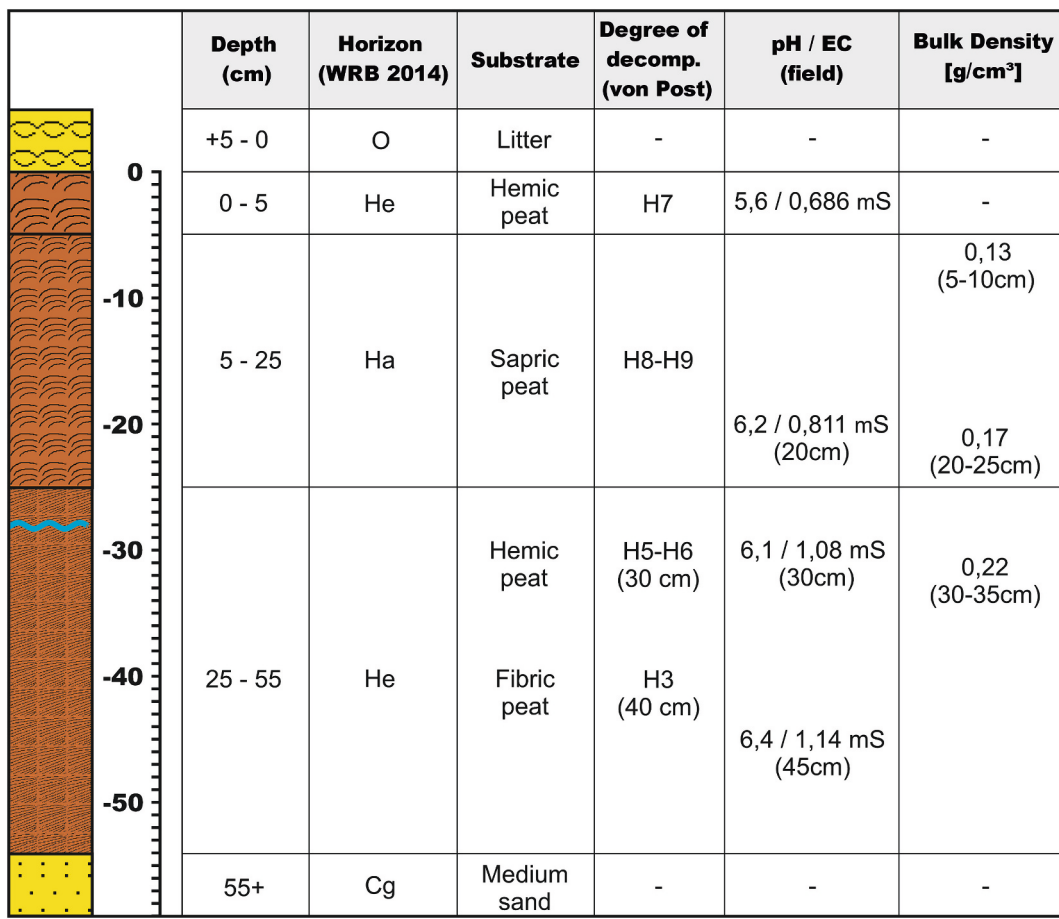


Fig. 2. Soil profile and soil field parameters. Blue line in the soil profile indicates water level at the time of the soil description, at 28 cm below ground. Degree of peat decomposition in WRB and Von Post (1922). (For interpretation of the references to colour in this figure legend, the reader is referred to the web version of this article.)

at a single depth is provided in supplementary information (Supplementary Fig. S2). According to the CONISS analysis, four zone were distinguished (see dendrogram in supplementary material): K1: 49–25 cm; K2: 25–21 cm; K3: 21–3 cm; K4: 3–0 cm. A summary of the macrofossil and pollen results is given in Table 2.

3.4. Testate amoebae

Testate amoebae were very sparse and preservation was extremely poor, which may be related to the highly humified peat samples. However, a small number of testate amoebae specimens were encountered in the samples analysed. In total, 9 types of testate amoebae were encountered (Supplementary Table S2), all of them from 0 to 21 cm of depth. With such low numbers of tests, it was difficult to make any environmental statements.

3.5. Geochemical analysis

A total of 13 Elements were analysed by WD-XRF (see Fig. 6).

K1 (1070–1370 CE, 49–25 cm): S, and Fe had highest overall concentrations in this section. Elevated and steady concentrations of Al, Si, and Ti indicate presence of mineral matter.

K2 (1370–1470 CE, 25–21 cm): None of the investigated elements showed a distinct peak in this small section. Si tended to increase, while S and Fe tended to decrease in upward direction.

K3 (1470–1936 CE, 21–3 cm): Al, Ca, K, Mn, Si and Ti had highest concentrations in this section, indicating high abundance of mineral matter, such as sand or clay minerals. In the interval from 16 to 20 cm,

most elements' concentrations, except for Si, showed a distinctive drop, indicating the persistent presence of silicates. Such high concentrations of silicates may interfere with the FTIR based indices for peat quality, as indicated by a locally very low humification index at this depth (see below). S and Fe continue their simultaneous concentration changes until around 1800 CE (8 cm), after which Fe concentrations start to increase while S concentrations, as well as Mn and Ti slightly drop.

K4 (1936–2015 CE, 3–0 cm): Na, Mg, P, Cl, Zn had their highest overall concentrations in this section and Fe had a secondary peak again here near the surface.

3.6. Carbon, Nitrogen, Phosphate contents and peat quality

In the bottom profile section, in between 1070 and 1490 CE (48–20 cm) the carbon content lingers constantly between 27 % and 33 % (Fig. 7), confirming the high content of mineral matter.

Around 1490–1600 CE (20–16 cm) C content dropped to 21 %, coinciding with even higher mineral content (Al, Si, Ti; see above). Afterwards C content steadily increased again up to 42 % in the part younger than 1900 CE (0–4 cm). The C/N ratio at 1070–1200 CE (48–44) was around 20, coinciding with the finding of material of relatively weaker decomposition. C/N ratios ranged from 15 to 17, indicating stronger decomposition, throughout the rest of the peat profile above that depth. P was generally increasing towards the surface throughout the whole profile, while N concentrations were more constant along depth. Accordingly, ratios of N/P were constantly decreasing in upward direction.

Holocellulose contents or carbohydrate-like structures, as estimated

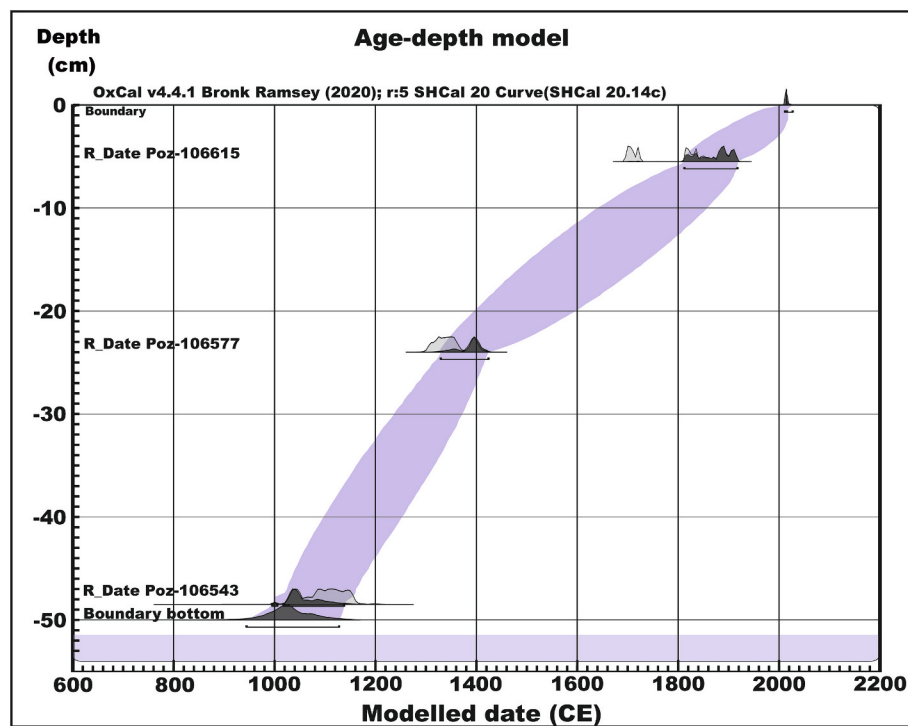


Fig. 3. Age-depth model, calculated with OxCal 4.4 (Bronk-Ramsey, 2009), calibrated using the SHCal20 atmospheric curve (Hogg et al., 2020) applying a P_Sequence function with a k-parameter of 1 cm^{-1} and 1-cm resolution.

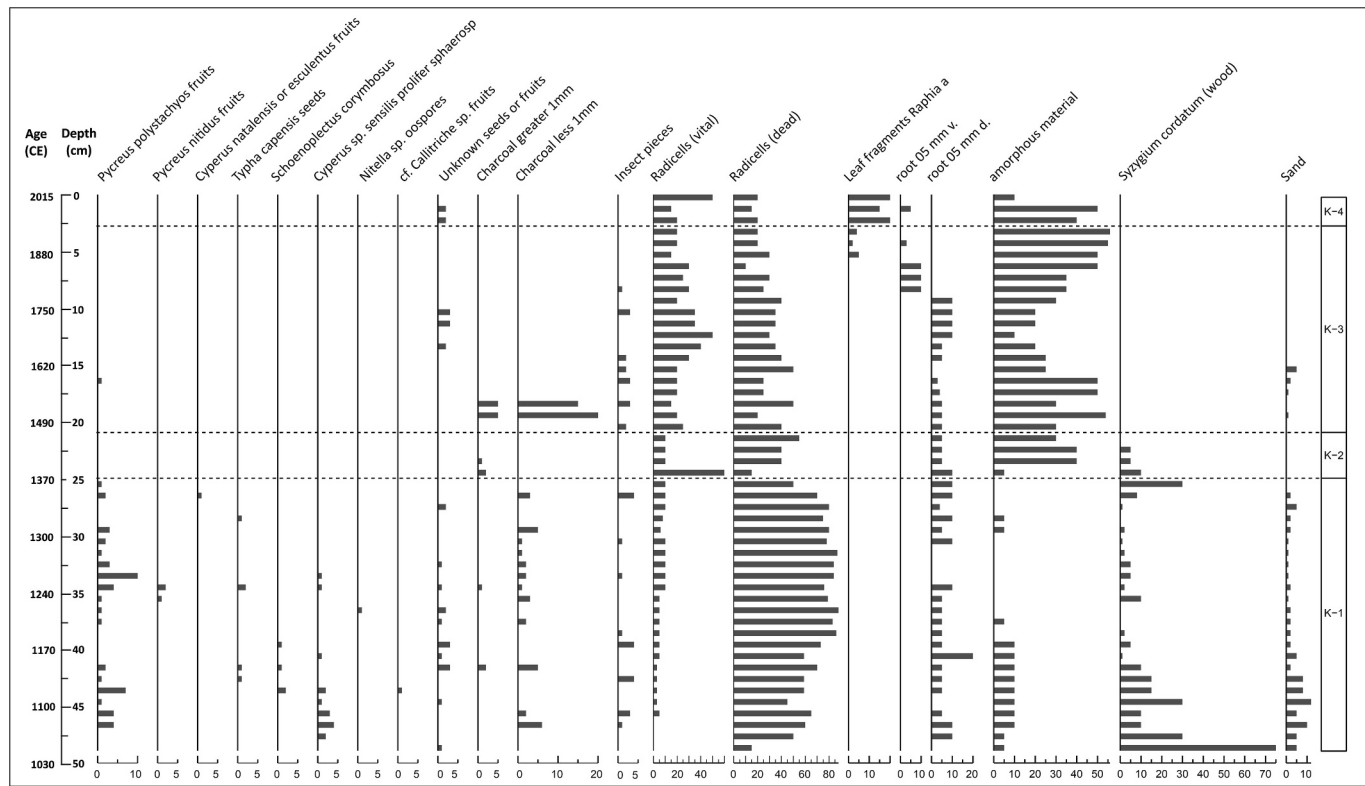


Fig. 4. Macrofossil diagram with macrofossils as individual counts, in vertical intervals of one cm. Quantitative estimations for radicells, roots, leaf fragments, amorphous organic matter, wood and sand are given in volumetric %, referring to remaining substance after wet sieving.

from FTIR spectra, were highest (0.3–0.42) at intermediate depths, corresponding with less decomposed peat following our soil description, and lowest (0.19–0.3) in the bottom and top parts of the profile. The

peak in 16–20 cm must be interpreted with care, though, due to the high presence of silicates interfering with spectral bands of carbohydrates. FTIR-derived Klason lignin contents or aromatic-like structures were

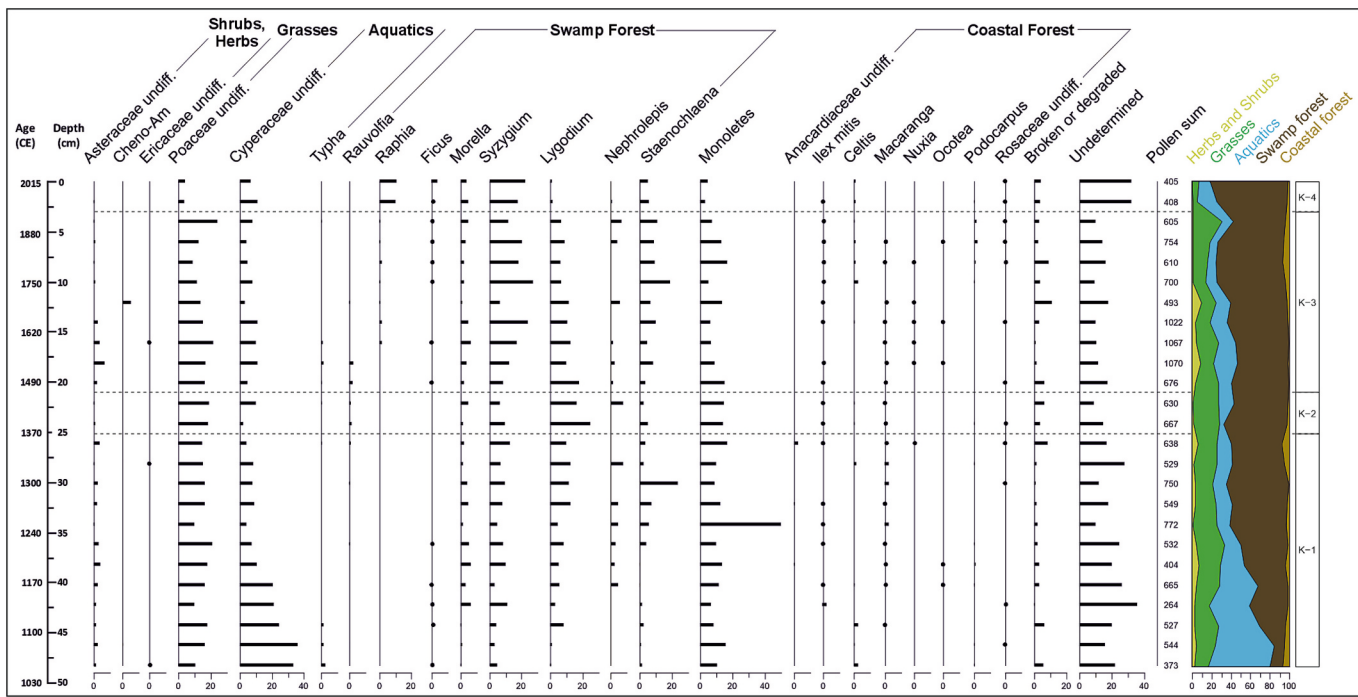


Fig. 5. Summary stratigraphic diagram of pollen of herbs and shrubs, grasses, aquatics, swamp forest and coastal forest, with total pollen sum and ecological group summary indicated on the far right. Rare taxa present at a single depth were excluded from the diagram.

almost uniform in the profile (0.26–0.29), except of an elevated content (0.47–0.49) in the top layer from 0 to 8 cm, corresponding with strongly decomposed peat, elevated P and N content, high abundance of aliphatics (Fig. 8), and with presence of visible remains of *Raphia* leaves.

The Humification Index (HI), ratios of absorption at wavenumbers 1630/1090, ranged from 0.5 to 0.86 almost in the entire peat profile and was inverse to FTIR-derived holocellulose content, as expected. Values were generally lower in the central section, corresponding with intermediately decomposed peat (36–12 cm) according to our lithological classification. Exceptions are a HI of 0.34 in the part from 1490 to 1600 CE (20–16 cm), which we attribute to interference of silicates due to their elevated content (Broder et al., 2012), and a HI of 1.25 in the part from 1900 CE to present day (4–0 cm), indicating strong enrichment of refractory aromatics over carbohydrates (also confirmed by absorption features around 600–900 cm^{-1}) (Stuart, 2004) (Fig. 8). Interestingly, the uppermost sample also had exceptionally high absorbance at 2890 and 2910 cm^{-1} , indicative of – similarly refractory – aliphatics (e.g. lipids) (Cocozza et al., 2003), but also sharp peaks around 1560, 1650, and 3300 cm^{-1} (Fig. 8) indicative of amids (Stuart, 2004). These sharp peaks of amids were only visible in the uppermost sample containing *Raphia* leaves, while below, where we identified roots and amorphous matter, amid peaks were largely absent or only present as shoulders of larger peaks (1560, 1650, and 3300 cm^{-1} , Fig. 8).

Vertical accumulation rates (VAR), carbon accumulation rates (CAR) (see also Fig. 7) and the long-term carbon accumulation rate (LORCA) are given in Table 3. The bulk densities for the radicell peat section was 0.22 g cm^{-3} (measured in 30–35 cm), whereas the *Raphia* peat had 0.13 g cm^{-3} (5–10 cm) and 0.17 g cm^{-3} (20–25 cm), respectively. For the calculation of carbon accumulation, a mean of 0.15 g cm^{-3} was used.

4. Discussion

4.1. Genesis of the *Raphia australis* peat swamp

The zonation made by CONISS fits well with the horizons of the soil profile description, except for zone k2, which has not shown any prominent characteristics to be distinguished in the field. The

macrofossil and pollen sequences show that the initial peat was accumulated by sedges. *R. australis* thus did not colonise bare mineral soil, like *R. taedigera* (Phillips, 1995), but colonised an already existing peatland, like known from *Mauritia flexuosa* in the Amazon (Kelly et al., 2020). The following section analyses the development chronologically.

4.1.1. 55–35 cm (970–1240 CE)

The radiocarbon dates indicate peat initiation begun around 970 CE, estimated for a peat depth of 55 cm with the given peat accumulation rate of the sedge peat (0.075 cm yr^{-1}). This fits into the pattern of rather recent initiations of coastal peatlands along the MCP (Elshehawi et al., 2019b), as consequence of late Holocene sea-level rise (Gabriel et al., 2017a; Grundling, 2004).

The initiation of the peatland occurred with Cyperaceae (Fig. 9) being the first peat-forming vegetation type (Fig. 10). The intermixtures of sand (see also Al, Si, Ti) indicate a more dynamic flood plain environment, even though the low degree of peat decomposition refers to permanently water saturated conditions.

During field description the bulk peat was assumed to be *Raphia* peat. Macrofossil analysis yet revealed it to be radicell peat from sedges, with intrusions of living and dead roots, originating from the recent *Raphia* palms. Macroscopically, these two peat types are difficult to differentiate, however, fruits and seeds of *Pycreus polystachyos*, *Pycreus nitidus*, *Cyperus* sp., *Schoenoplectus corymbosus*, and *Typha capensis* provided evidence of peat accumulation by sedge vegetation. Further, the high occurrence of *Pycreus polystachyos* underlines the findings of Gabriel et al. (2017a), who state that this species plays an important role for the formation of sedge peat in Maputaland.

The initiation of the peatland coincided with a warm and wet climate in the South African Summer Rain Zone around 1000 CE (Gabriel et al., 2017a; Lüning et al., 2018; Walther and Neumann, 2011; Woodborne et al., 2016). According to Lüning et al. (2018), a southern shift of the ITCZ by that time intensified tropical Easterlies in the region, and led to increased precipitation relative to the preceding period. A link between sea-level and the peatland initiation cannot be confirmed. The peatland initiation took place around 200 years after the sea-level of the South African East Coast dropped abruptly from its late Holocene High Stand

Table 2

Key findings of the palaeoenvironmental analysis.

Phase – Depth - Timing	Summary Macrofossils	Summary Pollen
K1 1050–1370 CE 49–25 cm	<u>Bulk peat</u> : Dead radicells (50–90 %) <u>Seeds/Fruits</u> : Mainly Cyperaceae, with five representatives. Most frequently <i>Pycreus polystachyos</i> , a total of 49 fruits. Fruits of <i>Cyperus</i> sp. were commonly encountered below 40 cm. One oospore of aquatic species <i>Nitella</i> sp. was found (36–37 cm). <u>Wood</u> : <i>Syzygium cordatum</i> (mostly between 49 and 40 cm) <u>Macrocharcoal</u> : Small pieces of <1 mm, in 13 of the 24 intervals – fire is a frequent feature throughout this phase	Sedge (Cyperaceae) pollen dominated the wetland system, with <i>Typha</i> reeds subdominant among the aquatic pollen taxa (Fig. 5). Swamp forest taxa, notably <i>Syzygium</i> , were sparsely represented relative to the remainder of the profile. Grass (Poaceae) pollen were well represented at frequencies of 10–15 %. From 1050 (49 cm) to 1240 CE (35 cm), Cyperaceae and <i>Typha</i> declined gradually, with swamp forest taxa showing a corresponding increase. Prominent swamp forest taxa included the tree species <i>Morella</i> and <i>Syzygium</i> and the epiphytic ferns <i>Lygodium</i> and <i>Nephrolepis</i> . The fern <i>Stenochlaena</i> began to increase later after ca. 1200 CE. Pollen of herbs and coastal forest occurred in low numbers.
K2 1370–1470 CE 25–21 cm	<u>Bulk peat</u> : Dead and vital radicells (approx. 40–60 %); amorphous matter (approx. 40 %). <u>Seeds/Fruits</u> : Absent <u>Wood</u> : Some <i>Syzygium cordatum</i> <u>Macrocharcoal</u> : Three pieces >1 mm in 23–25 cm	Swamp forest are firmly established at the site, with tree and fern taxa dominating the overall assemblage. <i>Stenochlaena</i> peaks first, followed by <i>Lygodium</i> and later <i>Syzygium</i> in the next zone. This may reflect successional processes with fern species acting as a precursor for the development of swamp forest trees such as <i>Syzygium</i> . <i>Nephrolepis</i> and <i>Morella</i> yet did not mirror this trend, being present throughout most of the record, and showing only slight variations in abundance. Grass (Poaceae) pollen occurred in the record constantly in a range of 10–15 %, while herbs and shrubs and coastal forest occurred in low numbers.
K3 1470–1936 CE 21–3 cm	<u>Bulk peat</u> : Amorphous material (mostly 30–50 %); Dead and vital radicells (mostly 40–50 %), fragments of <i>Raphia</i> leaves occurring from 6 cm upwards. <u>Seeds/Fruits</u> : Almost absent, except one <i>Pycreus polystachyos</i> and eight unknown seeds. <u>Wood</u> : Absent <u>Macrocharcoal</u> : High quantity of pieces both <1 mm and > 1 mm in 18–20 cm; absent in the rest of the section – no further fire events after 1544 CE (18 cm) upwards	After 1518 CE (19 cm), <i>Raphia</i> pollen were consistently recorded for the first time in the record, albeit at low frequencies. <i>Ficus</i> was also more consistently present after 1600 CE (16 cm). Among swamp forest taxa, <i>Syzygium</i> was dominant, along with fern spores from <i>Stenochlaena</i> and <i>Lygodium</i> well represented. A greater diversity of coastal forest taxa was present in the pollen assemblage, with trees <i>Podocarpus</i> , <i>Celtis</i> , and <i>Ilex mitis</i> becoming more prominent after 1700 CE.
K4 1936–2015 CE 3–0 cm	<u>Bulk Peat</u> : Amorphous material (approx. 40 %), dead and vital radicells (approx. 40 %), <i>Raphia</i> leaf fragments (approx. 20 %) <u>Seeds/Fruits</u> : Almost absent, except for four unknown seeds. <u>Wood</u> : Absent <u>Macrocharcoal</u> : Absent – no fire events	After 1936 CE, <i>Raphia</i> pollen became a dominant feature of the pollen diagram at frequencies of c. 10 %. Poaceae dropped off considerably, as did the ferns <i>Lygodium</i> and <i>Nephrolepis</i> . <i>Stenochlaena</i> declined similarly, but remained subdominant to <i>Syzygium</i> and <i>Raphia</i> . <i>Ficus</i> occurred in its highest frequencies of the profile, but remained poorly represented as a low pollen producer. Pollen of herbs and shrubs occurred in low numbers.

(about 1.5 m about today) to a sea-level about 0.5 m below the present-day level (Ramsay, 1995; Strachan et al., 2014). In contrast to most of the coastal peatlands on the MCP, we attribute wet climate conditions, and not sea-level rise (Elshehawi et al., 2019b), as the main driver for the formation of the peatland. Also, mobilisation and deposition of sediments, as described by Wright et al. (1997) and Cooper et al. (2012), might have altered the discharge in the Kosi Bay estuary. A possible lowering of the discharge with positive feedback on the water levels of the Siyadla River, could have given way to the peatland formation on the floodplain.

4.1.2. 35–25 cm (1240–1370 CE)

The macrofossil pattern of seeds and fruits of Cyperaceae and *Typha* indicate reed-sedge vegetation as peat builder. Wood remains of *Syzygium cordatum* in varying amounts (below 22 cm), confirm that this hardwood swamp forest species occurred at the actual study site, but according to the seed, fruit and charcoal record, it must be tree roots, grown in at a later stage, after 1370 CE (25 cm) (see 25–21 cm below). Pollen, however, indicates a general encroachment of swamp forest on the flood plain by a decline of semi-terrestrial species, mostly made of Cyperaceae, and a transition towards swamp forest.

Decreasing intermixture of sand and mineral matter in the peat indicate that the environment became more stable, after the establishment of the initial peat layer and the lateral expansion of it. The medium degree of peat decomposition (hemic), which is relatively higher than in 49–35 cm, following C/N ratios and HI, is likely to be caused by secondary decomposition. Two reasons are likely responsible for this. The aeration of the upper soil by presently abundant *R. australis* pneumatophores and more recent drop of water levels (see 21–3 cm).

4.1.3. 25–21 cm (1370–1470 CE)

The macrofossil record suggests a shift from open-reed sedge

peatland to hardwood swamp forest, mainly *Syzygium cordatum* (**Error! Reference source not found.**). Seeds of semi-terrestrial herbs are almost entirely absent in the peat younger than that age, and herbal undergrowth in swamp forests of the study region is very poor (Grobler, 2009). Further, there is a rise in wood content, around that depth. In addition, the constant occurrence of macrocharcoal only earlier than 1370 CE (25 cm) suggests that a closed swamp forest was not present, as fire is frequent during the dry season in open reed-sedge peatlands, but due to better preservation of humidity through shading and a lack of easy inflammable grass layer in the understory, it is uncommon in swamp forests (Gabriel et al., 2017a).

Especially indicative for this shift is the increase in spores from the epiphytic fern *Lygodium*. The macrofossil record similarly suggests a shift from a sedge dominated open peatland to a swamp forest around 1370 CE (25 cm).

4.1.4. 21–3 cm (1470–1936 CE)

A peak in macrocharcoal between 1490 and 1540 CE (20–18 cm) suggests a very big fire event, the largest fire event in the history of the peatland. As fire is a rare feature in swamp forest (Gabriel et al., 2017a), the fire was possibly related to an extreme drought. A dendrochronological study by Hall (1976) of a *Podocarpus* tree in the KwaZulu-Natal Midlands suggests a singular year of extreme dryness in 1508 CE, which might well coincide with the fire event evidenced in the macrofossil record. Nevertheless, even though Hall's study is widely cited, the direct connection between the *Podocarpus* tree ring width and climate drivers has never been verified. The higher levels of Si, Al, and Ti in 1490–1600 CE (20–16 cm) are likely derived from additional sand inputs after the fire. An alternative explanation, an enrichment of these elements by residuals from burnt peat has to be discarded, as the levels of other elements like Fe and Zn did not increase simultaneously in this depth section.

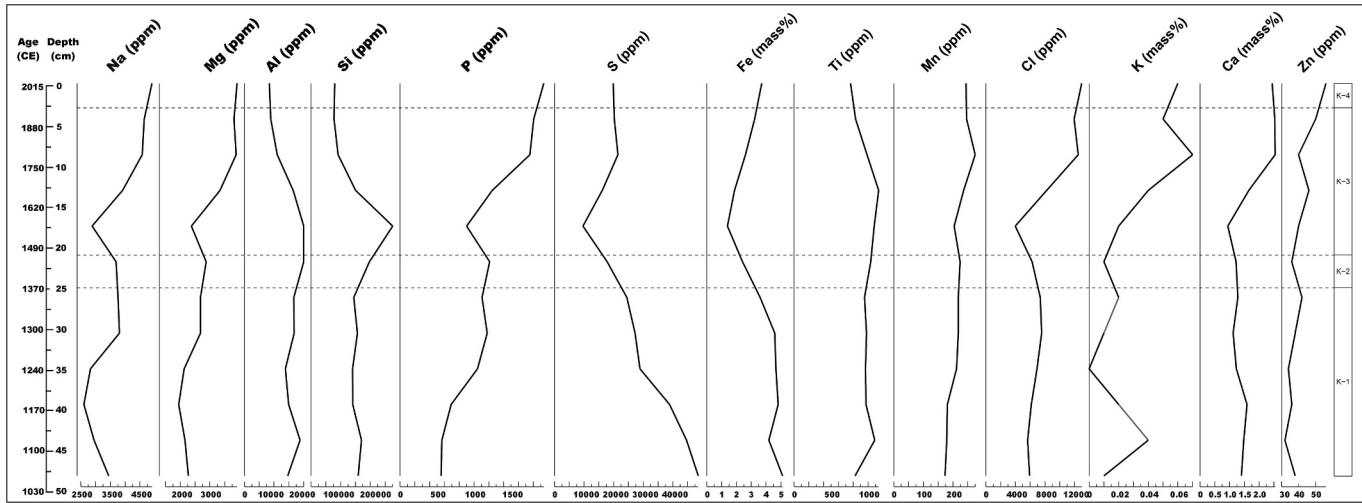


Fig. 6. X-ray fluorescence. Selected elements in parts per million (ppm, eq. to $\mu\text{g g}^{-1}$) or mass percent (mass%).

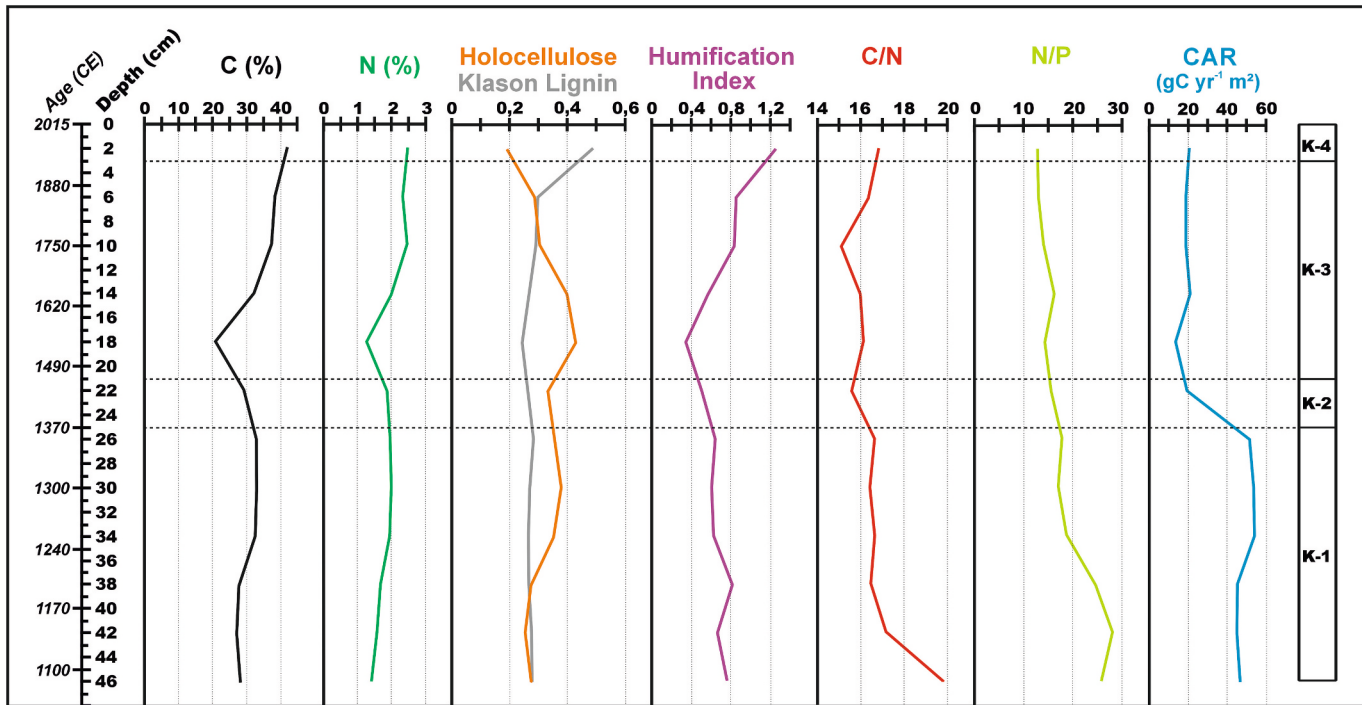


Fig. 7. Contents and elemental ratios of C, N, P, (as determined by XRF and elemental analysis), and carbon accumulation rate (CAR), humification index, and estimated holocelulose, and klason lignin contents (as derived by FTIR spectroscopy) (Hodgkins et al., 2018).

The presence of *R. australis* pollen after 1540 CE (above 18 cm) indicates that *Raphia* became established on the site after a large fire event (Fig. 9). This might well be a common pattern in the evolution of palm-swamp peatlands, as fire is also acknowledged to facilitate the *Mauritia flexuosa* colonisation (Rull and Montoya, 2014). The low quantity of *Raphia* pollen suggests a mixed swamp forest vegetation with *R. australis* and the hardwood species *Syzygium cordatum* and *Ficus trichopoda*. After 1800 CE (8 cm), the site became drier again, as evidenced by the increase in Fe in the capillary fringe and a simultaneous decrease in Mn and Ti (excluding mineral input as source of Fe). The almost parallel concentration changes of S and Fe between 48 cm and 8 cm within the mostly waterlogged part of the profile suggest that Fe may be present as Fe sulfides (FeS, FeS₂). Therefore, the Fe/Mn ratio, as a paleoredox indicator (Boyle, 2001), may be biased in our profile, given that the Fe concentration patterns appear to be determined rather by a change in

the predominant binding partner than by redox conditions. This pattern changes after 1800 CE, where opposite concentration trends of S and Fe are observed. We therefore interpret the increasing Fe concentrations, accompanied by decreasing Mn and Ti concentrations, as an indicator for currently more oxidizing conditions (Boyle, 2001), supporting the hypothesis of a currently drying trend at the site. Woodborne et al. (2016) reconstructed with $\delta^{13}\text{C}$ contents of tree rings a decline in precipitation for the summer rainfall region of South Africa throughout the Little Ice Age, beginning as early as 1580 CE. The pollen record suggests the dominance of *R. australis* at the site from approx. 1900 CE (4 cm) on. We strongly assume the vegetation evolved into today's homogenic *Raphia australis* stand by that time.

4.1.5. 3–0 cm (1936–2015 CE)

The surface peat exhibits a fairly low carbon accumulation rate

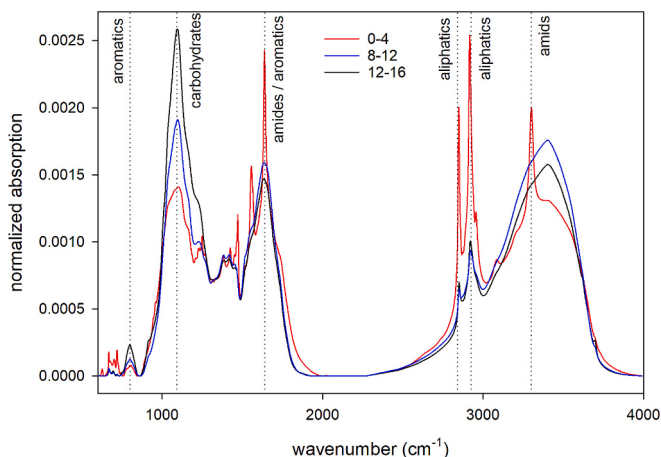


Fig. 8. Fourier transformed infrared (FTIR) spectra of *Raphia* bulk peat. Selected spectra are presented for uppermost peat (0–4 cm, red), dominated by *Raphia* leaf remains and amorphous matter, and two sections below (8–12 cm, blue; 12–16 cm, black), dominated by roots/root litter and amorphous matter (see also Fig. 4). Wavenumbers indicative of aromatics, carbohydrates, amides, and aliphatics are marked by dotted lines (following wavenumber ranges provided in Stuart (2004) and Broder et al. (2012)). (For interpretation of the references to colour in this figure legend, the reader is referred to the web version of this article.)

Table 3

Vertical Accumulation Rate (VAR), Carbon Accumulation Rate (CAR) and Longterm Carbon Accumulation (LORCA). *Raphia* peat is here referred to the peat substrate from 0 to 24 cm depth, as it forms as replacement peat by the ingrowth of roots into the topsoil (see chapter 4.1.).

	Sedge peat	Raphia peat	Entire site
Depth	48–25 cm	25–0 cm	48–0 cm
VAR	0,075 cm yr⁻¹	0,039 cm yr⁻¹	–
CAR	50 gC m² yr⁻¹	18 gC m² yr⁻¹	–
LORCA	–	–	28 gC m² yr⁻¹

(0.039 cm yr^{-1}). According to Succow and Jeschke (1986) peat accumulation in floodplain mires is linked to a rise of the river's water table. The low current rate of peat production, therefore, indicates that the continuous rise of water table levels in the Siyadla River slowed down in the last century. This is also reflected in the diverging concentration changes of Fe and Mn, i.e., higher Fe/Mn ratio (Boyle, 2001). Again, this is probably linked to a decline in precipitation, which is particularly pronounced from 1900 CE on (Woodborne et al., 2016). A continuation of this trend is likely. With anticipated higher temperatures ($1.5\text{--}3.5^\circ\text{C}$ until 2099), the associated increase of EVT and reduced rainfall ($-5\text{--}-10\%$ until 2099) (South African Weather Service, 2017), next to an increasing depletion of the ground water aquifers by *Eucalyptus* plantations in the recharge area (Von Roeder, 2015), peat accumulation might come to a standstill.

4.2. Peat characteristics

Based on the ratio of aromatics to carbohydrates of peat, Hodgkins et al. (2018) conclude that peat accumulation in low latitudes ($<45^\circ$) is favoured by the accumulation of more recalcitrant parent plant material, richer in aromatics and poorer in carbohydrates, in comparison to the high latitudes ($>45^\circ$). Thus, peat can also form in tropical places with high temperatures and water table fluctuations favouring microbial activity. Due to possible limitations in the exact calculations of the Klason lignin and Holocellulose fractions (Teickner and Knorr, 2022), we rather refer to aromatics and carbohydrates and limit our interpretation to observed relative changes, humification indices, and C/N

ratios. The composition of the *R. australis* peat does not show particularly high humification indices, but the surface layers (0–8 cm) show specific features indicative of a high share of aromatics, aliphatics, and also of amides (Broder et al., 2012; Stuart, 2004) (Fig. 6). Such high absorption bands indicative of aliphatics have also been reported for other *Raphia* palm leaves used to produce fibres (Elenga et al., 2009; Oliveira Filho et al., 2020), while the strong absorption features indicative of amides were surprising and have not been reported so far to the best of our knowledge. Just below that depth, the humification index decreases despite comparatively low C/N ratios, and peat quality changes substantially. Here, absorption bands indicative of aliphatics and amides strongly diminish, along with a shift from leaf-dominated peat to root/amorphous matter dominated peat. There is thus strong decomposition and alteration of the *Raphia* leaves in the peat, yet due to the changes in the peat parent vegetation this may not be easily distinguished in our profile based on C/N ratios of humification indices alone. In *Raphia* peat, the strong absorption indicative of refractory aliphatics may also evidence intermixtures of litter rich in wax compounds. Hoyos-Santillan et al. (2015) showed in decomposition experiments with *R. taedigera* in Panama that especially stems and leaves decay rapidly at the surface, with about 20 % of the initial biomass remaining after 24 months. The roots, however, containing three times more lignin than the leaves and twice as much as the stems, lost belowground only about 20 % of the initial biomass after 24 months (Hoyos-Santillan et al., 2015). As we used the deepest piece of *Raphia* leaf for radiocarbon dating, we can hereby state that in our case leaves become decomposed to a state beyond macroscopic recognisability after about 100 years, coinciding with the decrease of aliphatics and amids in the older material.

The fire event between 1490 and 1540 CE (20–18 cm) gave place to the establishment of *R. australis* on the site, like also observed for *M. flexuosa* successions in the Amazon (Rull and Montoya, 2014). The pollen record suggests mixed *Raphia*-hardwood swamp forest afterwards. Based on the *Raphia*-radicells in macrofossil record, we assume that *R. australis* was the main peat producing plant on the site since that date. Also, during the soil profile description, little wood intermixtures haven been recorded in the Ha horizon (FAO, 2015). As *R. australis* produces “replacement peat” (sensu Barthelmes et al., 2006), with a great share of the peat accumulating not at the surface, but in the soil underneath, the change between *Raphia* peat and sedge peat is visible in 25 cm. In contrast to the fibric-hemic (low to medium decomposed) sedge peat in 49–25 cm, the *Raphia* peat of the upper 25 cm is sapric (highly decomposed), along with narrow C/N and N/P ratios, which was confirmed in the plant macrofossil record by the high amounts of amorphous plant matter of partly up to 60 %. In other parts of the world, *Raphia* peat has also been described as very sapric, for example the peat of *R. taedigera* in Panama (Phillips and Bustin, 1996). The higher degree of decomposition is likely to result from aerobic conditions in the rooting zone as oxygen is conducted into the soil through the pneumatophores (Obermeyer and Strey, 1969), a characteristic known from other oxygen conducting peat forming species like *Astelia pumila* and *Donatia fascicularis*, (Fritz et al., 2011). Hoyos-Santillan et al. (2016), conducted experiments showing that in two centimetres distance to the pneumatophores of *R. taedigera*, oxygen levels in the soil are still elevated. They further compared the CO₂ emissions from a control part of their study site to a part, where the *Raphia* palms had been cut. 100 days after setting up the experiment, the CO₂ emissions at the site without *Raphia* palms were up to two times lower, evidencing the stronger decomposition processes in the soil under *Raphia*, due to the breathing roots.

High decomposition at the *R. australis* site of this research is further supported by the relatively lower content of organic matter, when compared to other South African peat types (75–93 %) from Gabriel et al. (2017b). As a result, the recent peat is of highly refractory nature, e.g., with high contents of aromatics and aliphatic structures. The FTIR humification index broadly reflects this trend of higher decomposition

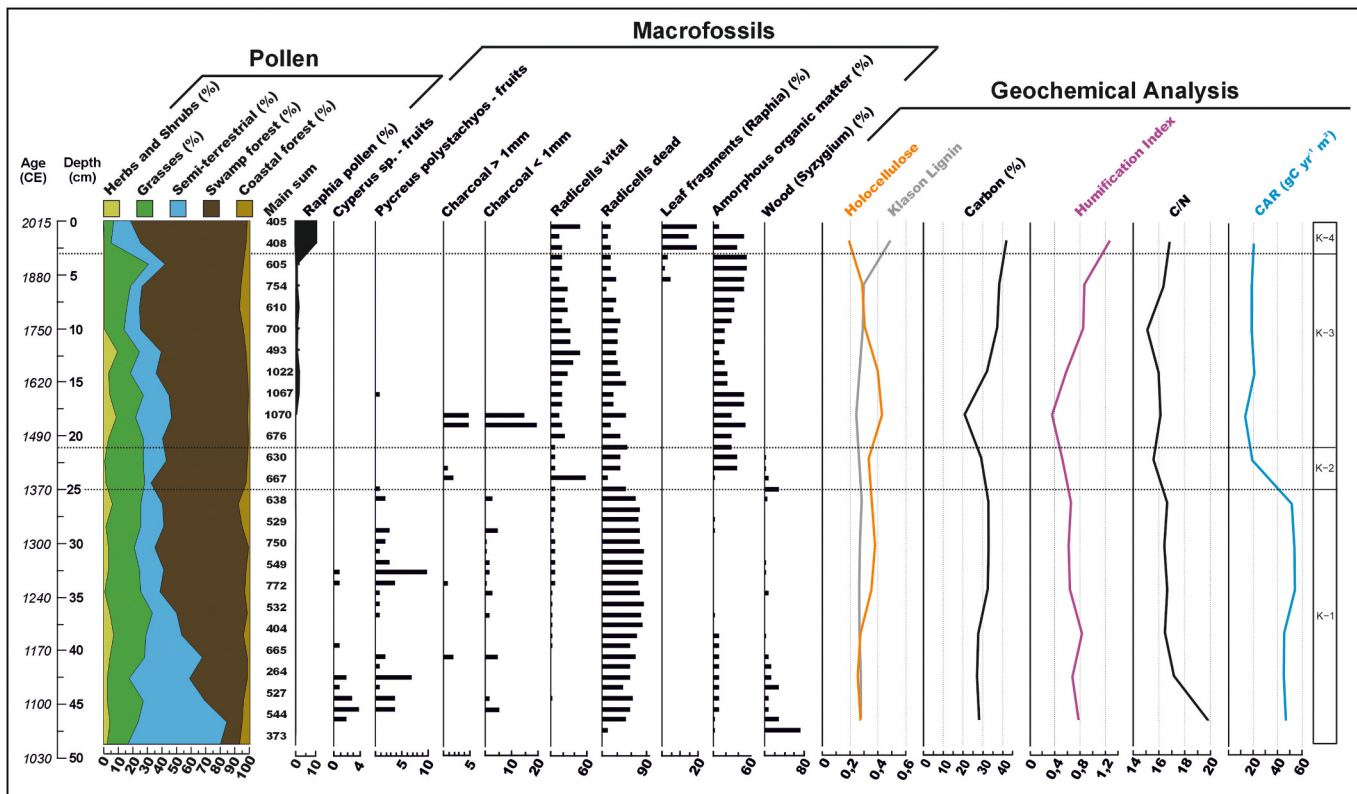


Fig. 9. Summary of pollen analysis, selected findings of the macrofossil analysis, and geochemical analysis.

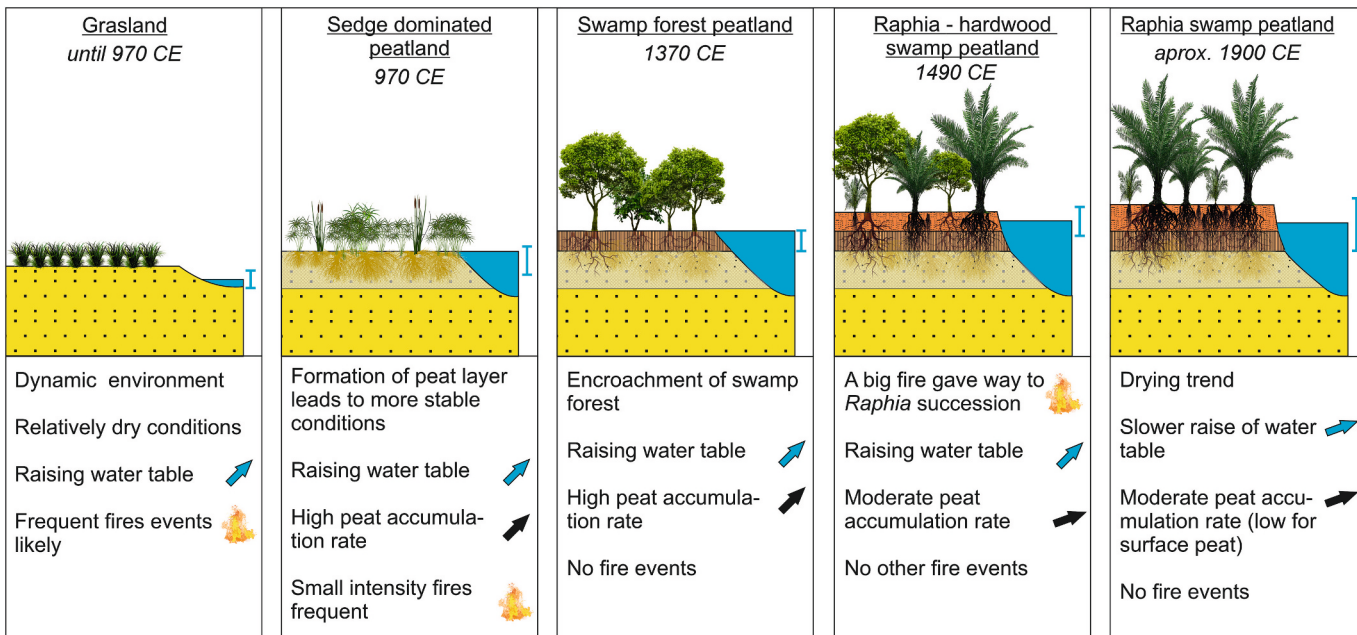


Fig. 10. Genesis of the *Raphia* swamp peatland at the floodplain of the Siyadla River. (Image was done using cliparts from “www.cleanpng.com”).

of the *Raphia* peat and lower decomposition of the radicell peat below. The minimum value of 0.34 between 1490 and 1600 CE (20–16 cm) has to be excluded, though, due to interference with high content of silicates (Broder et al., 2012). The FTIR humification index here is biased and cannot be interpreted. Silicates also absorb around the 1090 peak and therefore erroneously suggest a low HI.

A negative correlation between C/N ratio and the FTIR Humification

Index, as stated by Biester et al. (2014), where high C/N values correspond to low HI values, could not be confirmed in our study. We attribute this to the strongly contrasting vegetation in the past (sedges, swamp forest and *Raphia* palms). A deviation in these indices was already observed for profiles with shifts of contrasting types of vegetation (Mathijissen et al., 2019). However, still low ratios of C/N between 15 and 20 did correspond to our soil profile description of strongly

decomposed peat. These C/N ratios are lower than values generally reported for fens (24–32) (cf. Wang et al., 2015) and minerotrophic tropical peat swamps (20–25) (Watmough et al., 2022). The *Raphia* leaves identified in the surface peat must be subject to strong and rapid decomposition, as evident from the strongly differing FTIR spectra of surface peat (0–4 cm) versus the layers just below (8–16 cm) (Fig. 6). Compared to typical nutrient levels in Northern peat soils (Berger et al., 2017; Wang et al., 2015) and compared to levels of 1.4–2.0 % N and 550–1200 mg P kg⁻¹ in the sedge peat of the lower profile, the concentrations of macronutrients were much higher in the *Raphia* peat (2.0–2.5 % N and 1250–1940 mg P kg⁻¹). Moreover, high levels of Ca, Mg, Na, and K in the *Raphia* peat with high carbon content are presumably also due to strong decomposition and residual enrichment of these elements at the surface, while the lower carbon content in the sedge peat corresponds to elevated mineral content in this part of the profile, reflected by high levels of Al, Si, Fe, and Ti. The high Na and Cl levels in the upper soil can be attributed to sea-spray, due to the proximity of the ocean (Broder et al., 2015).

4.3. Carbon accumulation dynamics

Radiocarbon dating reveals distinct characteristics of peat accumulation for sedge peat (49–25 cm) and *R. australis* peat (25–0 cm). The 24 cm thick layer of sedge peat from sedges accumulated in 320 years (0.075 cm yr⁻¹), which is about 25 % lower than the average VAR of 0.106 cm yr⁻¹ (Grundling et al., 2000) stated for Maputaland. The accumulation of the 25 cm thick layer of *R. australis* peat took 640 years (0.039 cm yr⁻¹), with a rate of only 0.038 cm yr⁻¹ in the last century. Young et al. (2019) clarify that recent, near-surface peat, which has not undergone the same duration of decomposition process as older peat, usually yields particularly high apparent rates of carbon accumulation. Such rates not considering subsequent decomposition would be biased, so we conclude that peat formation processes are currently slowed down, possibly coming to stand still.

Compared to other South African peat substrates, usually ranging between 0.08 cm and 0.2 cm yr⁻¹, this is notably slower (Elshehawi et al., 2019c; Gabriel et al., 2017b; Grundling et al., 2000). A further distinction of the depth intervals of 25–5 cm and 5–0 cm within the *Raphia* peat shows a constant VAR of 0.039 cm yr⁻¹, and 0.038 cm yr⁻¹ respectively. Further, the carbon accumulation rate (CAR) of *R. australis* peat with 19 gC m⁻² yr⁻¹ is rather low, compared to those Gabriel et al. (2017a) determined for sedge peat (26–62 gC m⁻² yr⁻¹) and wood peat (91 gC m⁻² yr⁻¹) in peatlands of the MCP. The CAR for the radicell peat in this study with 50 gC m⁻² yr⁻¹ lies well in the range of the values.

The long-term apparent rate of carbon accumulation (LORCA) over the entire peat profile yields 28 gC m⁻² yr⁻¹ and is rather low, compared to rates Gabriel et al. (2017a) determined in the same region for a 920 years old reed-sedge peatland (89 gC m⁻² yr⁻¹) and a 6300 years old swamp forest peatland (55 gC m⁻² yr⁻¹). In comparison to peatlands in other tropical regions, the LORCA is rather low, as well. On the first view, the results resemble those measured in the Congo Basin, where adjacent to hardwood swamp vegetation *Raphia laurentii* and *Raphia hookeri* were found on active peatlands. LORCA values of eight sites (ages from 7140 cal BP to 10,550 cal BP) range from 18 gC m⁻² yr⁻¹ to 33 gC m⁻² yr⁻¹ (Dargie et al., 2017). However, older peatlands have generally lower LORCA values, as with increasing age and peat thickness the decomposition rate of the carbon accumulating catotelm increases as well (Clymo et al., 1998). The same trend can be seen in South American palm-swamp peatlands. Lähteenoja et al. (2009, 2012) report LORCA values for *M. flexuosa* peatlands of the Peruvian Amazon (2040 cal BP = 39 gC m⁻² yr⁻¹, 2300 cal BP = 74 gC m⁻² yr⁻¹, 2850 cal BP = 85 gC m⁻² yr⁻¹, 4500 cal BP = 36 gC m⁻² yr⁻¹, 7980 cal BP = 39 gC m⁻² yr⁻¹). In this context, the LORCA of the *R. australis* peatland, is remarkably low, considering its young age of about 970 CE. As *M. flexuosa* is also known to have pneumatophores (Hergoualc'h et al., 2024), it becomes clear that the low carbon accumulation rate of the *R. australis* site is not

only due to the breathing roots, but combined with the already mentioned change to a drier climate (Woodborne et al., 2016).

4.4. Ecological conditions of *Raphia australis* habitat

Comparing the *R. australis* swamp forest to the other peatland types of the MCP, it has rather unique characteristics. It's subneutral pH_{H2O} around 6 is much higher, than that of common reed-sedge fens or swamp forest peatlands of the lower part of the MCP, which exhibit acid pH_{H2O} values between 4 and 5 (Gabriel et al., 2017b). Also, the eutrophic peat properties with C/N ratio of 15–17, are not typical for the MCP either, whose peatlands are usually mesotrophic (20–33) (Gabriel et al., 2017b). This enrichment with N partly results from strong decomposition, due to the pneumatophores, next to the assumed lower water levels, especially throughout the last century (Woodborne et al., 2016). Also, the N/P ratio of 13–16 in *Raphia* peat is much lower than values known from northern peatlands, e.g. 26 in fens and 37 in swamps (Wang et al., 2015), indicating also strong enrichment of P and rather no P limitation at this site. Unfortunately, data for direct comparison with other peatlands of the MCP is lacking.

Compared with the *Raphia* peatlands in the Congo Basin from Dargie (2015), these have much lower pH values (2.7–3.2) and much lower electrical conductivities of approx. 0.15–0.222 mS. The high conductivities in Kosi Bay of 0.69–1.1 mS can be explained by proximity to the ocean and inputs from sea spray. However, these findings point out that *Raphia* as a genus has a certain tolerance or ecological range. The low pH values in the Congo peatlands can be explained by the high supply of precipitation water in the inner tropics, compared to the purely groundwater-fed peatlands of the MPC. Unfortunately, the ecological range of *R. australis* in terms of pH and EC could not be assessed further, due to a single study site. In a broader comparison of palm-swamp peatlands, the *R. australis* swamp is much closer to *Mauritia flexuosa* dominated palm-swamps peatlands of the Amazon, where Lähteenoja et al. (2012) measured pH values of 5.1–6.1 and C/N ratios of 17.9–20.9 in 5 peatlands. Further, many *M. flexuosa* peatlands share the same hydrogeomorphic type, as they also typically originated on flood plains of the Amazon and tributaries (Lähteenoja and Page, 2011). Also, *M. flexuosa* tends to form monodominant stands on waterlogged substrates. However, in contrast to *R. australis*, which today covers only small areas, *M. flexuosa* peatlands are more extensive and they are considered a main peat builder in the Amazon (Householder et al., 2012).

Unfortunately, no precise information can be given about the hydrological site conditions in Kosi Bay due to a lack of measurements. The lack of well-preserved testate amoebae, in addition, disappointed expectations of reconstructing past water levels. For *Raphia* swamp peatlands in the Congo Basin, Dargie (2015) measured mean water levels of –0.05 m, as well as minimum levels of –0.41 m and maximum levels of 0.25 m. Grobler (2009) saw *Raphia australis* swamp forest of the MCP as the drier peat swamps, whereas hardwood dominates the wetter parts, indicating *Raphia*'s inferiority to *Syzygium cordatum*, *Ficus trichopoda* and *Voacanga thouarsii*, when it becomes wetter.

5. Conclusions

R. australis did not initiate peat formation, but colonised an already existing peatland. Peat forming parts are the roots, leaves become decomposed rapidly at the surface. *R. australis* stands, apparently accumulate peat at a slow rate. The peat is more decomposed than in other tropical peat swamp forests, likely due to the preference of slightly dryer habitats and the oxygenating effect of the pneumatophore roots.

For mapping campaigns, *R. australis*, and probably other *Raphia* species, in other parts of the world, could be considered as an indicator for peatlands with decomposed surface peat.

Peat formation at the study site slowed down in the last centuries. The limits for peatland growth on the flood plain might be reached soon,

as the groundwater fed river will likely suffer reduced recharge with predicted increasing evapotranspiration and reduced precipitation.

Ecologically, *Raphia australis* habitat resembles more that of *Mauritia flexuosa* palm-swamps in South America than palm-swamps of other *Raphia* species in the Congo Basin. The ecological/trophic situation at the floodplain of the Siyadla River is quite unique for the lower Maputaland Coastal Plain. Fortunately, the area is protected by the iSimangaliso Wetland Park.

Supplementary data to this article can be found online at <https://doi.org/10.1016/j.palaeo.2025.113217>.

CRediT authorship contribution statement

Marvin Gabriel: Writing – original draft, Methodology, Investigation, Formal analysis, Conceptualization. **Jemma Finch:** Writing – review & editing, Writing – original draft, Methodology, Investigation, Conceptualization. **Klaus-Holger Knorr:** Writing – original draft, Methodology, Formal analysis. **Amanda Khuzwayo:** Writing – original draft, Formal analysis. **Graeme T. Swindles:** Writing – original draft, Methodology. **Mariusz Gałka:** Writing – original draft, Methodology.

Declaration of competing interest

The authors declare the following financial interests/personal relationships which may be considered as potential competing interests: (Marvin Gabriel reports financial support was provided by German Academic Exchange Service. Mariusz Gałka reports financial support was provided by National Science Centre Poland. If there are other authors, they declare that they have no known competing financial interests or personal relationships that could have appeared to influence the work reported in this paper.)

Acknowledgements

The idea of this research arose subsequently to the research activities of the DAAD project: Alliance for Wetlands – Research and Restoration (AliWET-RES) 2012-2015 (project no. 55516208), Piet-Louis Grundling and Jan Sliva are thanked on this occasion for initiating this project and DAAD for funding it. Thanks to Nhlanhla Masinga, Niko Roßkopf and Franziska Faul (fieldwork). Radiocarbon dating was funded by the National Science Centre (Poland), grant no DEC-2013/09/B/ST10/01589 (PI:Mariusz Gałka). Thanks to Alison Young (UKZN Botanical Gardens) and Christina Curry (Bews Herbarium) for obtaining *R. australis* modern pollen reference material from the UKZN Botanical Garden. We thank Henning Teickner for assistance in FTIR data analysis and Daniel Brüggemann for laboratory support. We also would like to thank Thomas Kelly and one unknown reviewer for their recommendations, which improved the quality of this article.

Data availability

The authors confirm that all data necessary for supporting the scientific findings of this paper have been provided.

References

- Barthelmes, A., Prager, A., Joosten, H., 2006. Palaeoecological analysis of *Alnus* wood peats with special attention to non-pollen palynomorphs. *Rev. Palaeobot. Palynol.* 141, 33–51. <https://doi.org/10.1016/j.revpalbo.2006.04.002>.
- Begg, G.W., 1980. The Kosi System: Aspects of its biology, management and research. In: Bruton, M., Cooper, K. (Eds.), *Studies on the Ecology of Maputaland*. Cape and Transvaal Printers, Cape Town, pp. 358–373.
- Bennett, B., 2009. Psimpoll 4.27: C program for plotting and analysis of palaeoecological data. Available online from Queen's University of Belfast, Department of Archaeology and Palaeoecology. <http://www.chrono.qub.ac.uk/psimpoll/psimpoll.html> (accessed 25th June 2025).
- Berger, S., Gebauer, G., Blodau, C., Knorr, K.-H., 2017. Peatlands in a eutrophic world - Assessing the state of a poor fen-bog transition in southern Ontario, Canada, after long term nutrient input and altered hydrological conditions. *Soil Biol. Biochem.* 114, 131–144. <https://doi.org/10.1016/j.soilbio.2017.07.011>.
- Biester, H., Knorr, K.-H., Schellekens, J., Basler, A., Hermanns, Y.M., 2014. Comparison of different methods to determine the degree of peat decomposition in peat bogs. *Biogeosciences* 11, 2691–2707. <https://doi.org/10.5194/bg-11-2691-2014>.
- Bocko, Y.E., Loubota, G.J., Dargie, G.C., Wenina Mampouya, Y.E., Mbemba, M., Loumete, J.J., Lewis, S.L., 2023. Allometric equation for *Raphia laurentii* De Wild, the commonest palm in the Central Congo peatlands. *PLoS One* 1–15. <https://doi.org/10.1371/journal.pone.0273591>.
- Boden, Ad-hoc-AG, 2005. Bodenkundliche Kartieranleitung – 5. Bundesanstalt für Geowissenschaften und Rohstoffe, Hannover (in German).
- Booth, R., Lamentowicz, M., Charman, D., 2010. Preparation and analysis of testate amoebae in peatland paleoenvironmental studies. *Mires and Peat* 7 (02), 1–7.
- Bord na Móna, 1985. Fuel Peat in developing Countries. In: World Bank Technical Paper Number 41. The World Bank, Washington DC.
- Botha, G., Porat, N., 2007. Soil chronosequence development in dunes on the southeast African coastal plain, Maputaland, South Africa. *Quat. Int.* 162–163, 111–132. <https://doi.org/10.1016/j.quaint.2006.10.028>.
- Boyle, J.F., 2001. Inorganic geochemical methods in palaeolimnology. In: Last, W.M., Smol, J.P. (Eds.), *Tracking Environmental Change Using Lake Sediments, Physical and Geochemical Methods*. Kluwer Acad. vol. 2. Publishers, Dordrecht, pp. 83–141.
- Broder, T., Blodau, C., Biester, H., Knorr, K.H., 2012. Peat decomposition records in three pristine ombrotrophic bogs in southern Patagonia. *Biogeosciences* 9, 1479–1491. <https://doi.org/10.5194/bg-9-1479-2012>.
- Broder, T., Blodau, C., Biester, H., Knorr, K.H., 2015. Sea spray, trace elements, and decomposition patterns as possible constraints on the evolution of CH₄ and CO₂ concentrations and isotopic signatures in oceanic ombrotrophic bogs. *Biogeochemistry* 122 (2–3), 327–342. <https://doi.org/10.1007/s10533-014-0044-5>.
- Bronk-Ramsey, C., 2009. Bayesian analysis of radiocarbon dates. *Radiocarbon* 51 (1), 337–360. <https://doi.org/10.1017/S0033822200033865>.
- Clymo, R.S., Turunen, J., Tolonen, K., 1998. Carbon Accumulation in Peatlands. *Oikos* 81 (2), 368–388. <https://doi.org/10.2307/3547057>.
- Cocozza, C., D'Orazio, V., Miano, T.M., Shotyk, W., 2003. Characterization of solid and aqueous phases of a peat bog profile using molecular fluorescence spectroscopy, ESR and FT-IR, and comparison with physical properties. *Org. Geochem.* 34, 49–60. [https://doi.org/10.1016/S0146-6380\(02\)00208-5](https://doi.org/10.1016/S0146-6380(02)00208-5).
- Cook, C.D., 2004. *Aquatic and Wetland Plants of Southern Africa*. Backhuys Publishers, Leiden.
- Cooper, J.A.G., Green, A.N., Wright, C.I., 2012. Evolution of an incised valley coastal plain estuary under low sediment supply: a 'give-up' estuary. *Sedimentology* 59, 899–916. <https://doi.org/10.1111/j.1365-3091.2011.0284.x>.
- Dargie, G.C., 2015. *Quantifying and Understanding the Tropical Peatlands of the Central Congo Basin*. PhD Thesis., University of Leeds, p. 268.
- Dargie, G.C., Lewis, S.L., Lawson, I.T., Mitchard, E.T.A., Page, S.E., Bocko, Y.E., Ifo, S.A., 2017. Age, extent and carbon storage of the Central Congo Basin peatland complex. *Nature* 542, 86–90. <https://doi.org/10.1038/nature21048>.
- DIN EN 15934: 2012-11. Deutsche Industrie Norm: Schlamm, behandelter Bioabfall, Boden und Abfall – Berechnung des Trockenmassanteils nach Bestimmung des Trockenrückstands oder des Wassergehalts; Deutsche Fassung (in German).
- Elenga, R.G., Dirras, G.F., Goma Maniongui, J., Djemia, P., Biget, M.P., 2009. On the microstructure and physical properties of untreated *Raffia textilis* fiber. *Compos. A: Appl. Sci. Manuf.* 40 (4), 418–422. <https://doi.org/10.1016/j.compositesa.2009.01.001>.
- Elshehawi, S., Barthelmes, A., Beer, F., Joosten, H., 2019a. Assessment of Carbon (CO₂) emissions avoidance potential from the Nile Basin peatlands Technical Report NBI Technical reports - WRM 2019-13. <https://nilebasin.org/index.php/informationhub/technical-documents/83-asessment-of-carbon-co2-emissions-avoidance-potential-from-the-nile-basin-peatlands>.
- Elshehawi, S., Grundling, P.L., Gabriel, M., Grootjans, A.P., Van der Plicht, J., 2019b. South African peatlands: a review of late Pleistocene-Holocene developments using radiocarbon dating. *Mires and Peat* 24 (11), 1–14. <https://doi.org/10.19189/MaP.2019.KHR.329>.
- Elshehawi, S., Grundling, P.L., Gabriel, M., Pretorius, L., Bukhosini, S., Butler, M., Van der Plicht, J., Grundling, P.L., Grootjans, A., 2019c. Ecohydrological assessment of the Vasi peatland complex in South Africa indicates degradation driven by changes in land use. *Mires and Peat* 24 (33), 1–21. <https://doi.org/10.19189/MaP.2019.OMB STA.1815>.
- Faegri, K., Iverson, J., 1989. *Textbook of Pollen Analysis*. John Wiley and Sons, Chichester.
- FAO, 2015. World Reference Base for Soil Resources - International soil classification system for naming soils and creating legends for soil map. *World Soil Res. Rep.* 106. Rome, 203 pp. E-ISBN 978-92-5-108370-3.
- Filho, Oliveira, Ei, G.D., Luz, F.S.D., Fujiyama, R.T., Silva, A.C.R.D., Cândido, V.S., Monteiro, S.N., 2020. Effect of Chemical Treatment and Length of Raffia Fiber (*Raffia vinifera*) on Mechanical Stiffening of Polyester Composites. *Polymers* 12, 2899. <https://doi.org/10.3390/polym12122899>.
- Fritz, C., Pancotto, V.A., Elzenga, J.T., Visser, E.J., Grootjans, A.P., Pol, A., Iturraspe, I., Roelofs, J.G., Smolders, A.J., 2011. Zero methane emission bogs: extreme rhizosphere oxygenation by cushion plants in Patagonia. *New Phytol.* 190 (2), 398–408. <https://doi.org/10.1111/j.1469-8137.2010.03604.x>.
- Gabriel, M., 2019. Peatlands in Maputaland: Genesis, Substrates and Properties Exemplified by the Region of "Greater Mangazi" – A Basis for Recommendations on Sustainable Cultivation, Conservation and Restoration. PhD Thesis. Humboldt-Universität zu Berlin, Berlin, Germany. <http://edoc.hu-berlin.de/18452/20674> (accessed 13 January 2025).

- Gabriel, M., Gaika, M., Pretorius, M.L., Zeitz, J., 2017a. The development pathways of two peatlands in South Africa over the last 6200 years: implications for peat formation and palaeoclimatic research. *The Holocene* 27 (10), 1499–1515. <https://doi.org/10.1177/0959683617693896>.
- Gabriel, M., Toader, C., Faul, F., Roßkopf, N., van Husyssteen, C.W., Grundling, P.L., Zeitz, J., 2017b. Peatland substrates in northern KwaZulu-Natal – the forming environments, the properties and an approach towards the classification. *S. Afr. J. Plant Soil* 35 (29), 149–160. <https://doi.org/10.1080/02571862.2017.1360950>.
- Gabriel, M., Toader, C., Faul, F., Roßkopf, N., Grundling, P.L., Grundling, A., van Husyssteen, C., Zeitz, J., 2018. Physical and hydrological properties of peat as proxies for degradation of South African peatlands – Implications for conservation. *Mires and Peat* 21 (23), 1–21. Doi: [10.19189/MaP.2018.OMB.336](https://doi.org/10.19189/MaP.2018.OMB.336).
- Gordon-Gray, K.D., 1995. *Cyperaceae in Natal. Strelitzia 2.* National Botanical Institute, Pretoria.
- Grimm, E.C., 1987. CONISS: a FORTRAN 77 program for stratigraphically constrained cluster analysis by the method of incremental sum of squares. *Comput. Geosci.* 13, 13–35. [https://doi.org/10.1016/0098-3004\(87\)90022-7](https://doi.org/10.1016/0098-3004(87)90022-7).
- Grobler, R., 2009. *A Phytosociological Study of Peat Swamp Forests in the Kosi Bay Lake System, Maputaland.* Thesis, University of Pretoria, South Africa, South Africa. MSC.
- Grobler, R., Moring, C., Sliva, J., Bredenkamp, G., Grundling, P.L., 2004. Subsistence farming and conservation constrains in coastal peat swamp forests of the Kosi Bay Lake system, Maputaland, South Africa. *Géocarrefour* 79 (4), 216–324. <https://doi.org/10.4000/geocarrefour.842>.
- Grundling, P.L., 2004. The role of sea-level rise in the formation of Peatlands in Maputaland. South Africa. <https://aquadocs.org/handle/1834/703> (accessed 23 December 2016).
- Grundling, P.L., Mazus, H., Baartman, L., 1998. Peat Resources of Northern KwaZulu-Natal Wetlands: Maputaland. Department of Environmental Affairs and Tourism, Pretoria.
- Grundling, P.L., Baartman, L., Mazus, H., Blackmore, A., 2000. Peat Resources of KwaZulu-Natal Wetlands: Southern Maputaland and the North and South Coast (Council for Geoscience report 2000-0132). Department of Environmental Affairs and Tourism, Pretoria.
- Hall, M., 1976. Dendroclimatology, Rainfall and Human Adaptation in the later Iron Age of Natal and Zululand. *Ann. Natal Museum* 22 (3), 693–703. <https://hdl.handle.net/10520/AJA03040798.617>.
- Hawthorne, D., Lawson, I.T., Dargie, G.C., Bocko, Y.E., Ifo, S.A., Garcin, Y., Schefuß, E., Hiles, W., Jovani-Sancho, A.J., Tyrell, G., Biddulph, G.E., Boom, A., Chase, B.M., Gulliver, P., Page, S.E., Roucoux, K.H., Sjögersten, S., Young, D.M., Lewis, S.L., 2023. Genesis and development of an interfluvial peatland in the Central Congo Basin since the late Pleistocene. *Quat. Sci. Rev.* 305 (107992), 1–24. <https://doi.org/10.1016/j.quascirev.2023.107992>.
- Helmstetter, A., Mogue Kamga, S., Bethune, K., Lautenschläger, T., Zizka, A., Bacon, C. D., Wiering, J.J., Stauffer, F., Antonelli, A., Sonké, B., Couvreur, T.L., 2020. Unravelling the Phylogenomic Relationships of the Most Diverse African Palm Genus *Raphia* (Calamoideae, Arecaceae). *Plants* 9 (549), 1–20. <https://doi.org/10.3390/plants9040549>.
- Hergoualc'h, K., van Lent, J., Dezzeo, N., Verchot, L., van Groenigen, J.W., López Gonzales, M., Grandez-Rios, J., 2024. Major carbon losses from degradation of Mauritia flexuosa peat swamp forests in western Amazonia. *Biogeochemistry* 167, 327–345. <https://doi.org/10.1007/s10533-023-01057-4>.
- Hodgkins, S.B., Richardson, C.J., Dommain, R., Hongjun, W., Glaser, P.H., Verbeke, B., Winkler, B.R., Cobb, A.R., Rich, V.I., Missilmani, M., Flanagan, N., Ho, M., Hoyt, A. M., Harvey, C.F., Vining, S.R., Hough, M.A., Moore, T.R., Richard, P.J., De La Cruz, F.B., Toufaily, J., Hamdan, R., Cooper, W.T., Chanton, J.P., 2018. Tropical peatland carbon storage linked to global latitudinal trends in peat recalcitrance. *Nat. Commun.* 9 (1), 3640. <https://doi.org/10.1038/s41467-018-06050-2>.
- Hogg, A.G., Heaton, T.H., Hua, Q., Palmer, J., Turney, C., Southon, J., Bayliss, A., Blackwell, P., Boswijk, G., Bronk Ramsey, C., Pearson, C., Petchey, F., Reimer, P.J., Reimer, R., Wacker, L., 2020. SHCal20 Southern Hemisphere Calibration, 0–55,000 years cal BP. *Radiocarbon* 62 (4), 759–778. <https://doi.org/10.1017/RDC.2020.59>.
- Householder, J.E., Janovec, J.P., Tobler, M.W., Page, S., Lähteenoja, O., 2012. Peatlands of the Madre de Dios River of Peru: distribution, Geomorphology, and Habitat Diversity. *Wetlands* 32, 359–368. <https://doi.org/10.1007/s13157-012-0271-2>.
- Hoyos-Santillan, J., Lomax, B.H., Large, D., Turner, B.L., Boom, A., Lopez, O.R., Sjögersten, S., 2015. Getting to the root of the problem: litter decomposition and peat formation in lowland Neotropical peatlands. *Biogeochemistry* 126, 115–129. <https://doi.org/10.1007/s10533-015-0147-7>.
- Hoyos-Santillan, J., Craigon, J., Lomax, B., Lopez, O., Turner, B., Sjögersten, S., 2016. Root oxygen loss from *Raphia taedigera* palms mediates greenhouse gas emissions in lowland neotropical peatlands. *Plant Soil* 404 (1), 47–60. <https://doi.org/10.1007/s11104-016-2824-2>.
- Joosten, H., Clarke, D., 2002. Wise Use of Mires and Peatlands – Background and Principles Including a Framework for Decision-Making. International mire conversation group and International peat society, Saarjärvi, p. 304.
- Joosten, H., Sirin, A., Couwenberg, J., Laine, J., Smith, P., 2016. The role of peatlands in climate regulation. In: Bonn, A., Allot, T., Evans, M., Joosten, H., Stoneman, R. (Eds.), *Peatland Restoration and Ecosystem Services: Science, Policy and Practice*. Cambridge University Press, Cambridge, pp. 63–76. <https://doi.org/10.1017/CBO978113917788.005>.
- Juggins, S., 2007. *C2 Version 1.5 Software for ecological and palaeoecological data analysis and visualisation Newcastle upon Tyne.* Newcastle University.
- Kelly, T.J., Lawson, I.T., Roucoux, K.H., Baker, T.R., Honorio Coronado, E.N., 2020. Patterns and drivers of development in a west Amazonian peatland during the late Holocene. *Quat. Sci. Rev.* 230, 106168. <https://doi.org/10.1016/j.quascirev.2020.106168>.
- Kirpotin, S.N., Antoshkina, O.A., Berezin, A.E., Elshehawi, S., Feurdean, A., Lapshina, E. D., Pokrovsky, O.S., Peregon, A.M., Semenova, N.M., Tanneberger, F., Volkov, I.V., Volkova, I.I., Joosten, H., 2021. Great Vasyugan Mire: how the world's largest peatland helps addressing the world's largest problems. *Ambio* 50, 2038–2049. <https://doi.org/10.1007/s13280-021-01520-2>.
- Lähteenoja, O., Page, S., 2011. High diversity of tropical peatland ecosystem types in the Pastaza-Marañón basin, Peruvian Amazonia. *J. Geophys. Res.* 116 (G2), 1–14. <https://doi.org/10.1029/2010JG001508>.
- Lähteenoja, O., Ruokolainen, K., Schulman, L., Oinonen, M., 2009. Amazonian peatlands: an ignored C sink and potential source. *Glob. Chang. Biol.* 15, 2311–2320. <https://doi.org/10.1111/j.1365-2486.2009.01920.x>.
- Lähteenoja, O., Reátegui, Y.R., Räsänen, M., Del Castillo Torres, D., Oinonen, M., Page, S., 2012. The large Amazonian peatland carbon sink in the subsiding Pastaza-Marañón foreland basin, Peru. *Glob. Chang. Biol.* 18, 164–178. <https://doi.org/10.1111/j.1365-2486.2011.02504.x>.
- Lüning, S., Gaika, M., Bauchi Danladi, I., Aanuoluwa Adagunodo, T., Vahrenholt, F., 2018. Hydroclimate in Africa during the medieval climate Anomaly. *Palaeogeogr. Palaeoclimatol. Palaeoecol.* 495, 309–322. <https://doi.org/10.1016/j.palaeo.2018.01.025>.
- Matijsse, P.J.H., Gaika, M., Borken, W., Knorr, K.-H., 2019. Plant communities control long term carbon accumulation and biogeochemical gradients in a Patagonian bog. *Sci. Total Environ.* 684, 670–681. <https://doi.org/10.1016/j.scitotenv.2019.05.310>.
- Matimele, H.A., Massingue, A.O., Raimondo, D., Bandeira, S., Burrows, J.E., Darbyshire, I., Timberlake, J., 2016. *Raphia australis*. The IUCN Red List of Threatened Species 2016. <https://doi.org/10.2305/IUCN.UK.2016-3.RLTS.T30359A85955288.en> (accessed 12 December 2021).
- Mattson, M., Uken, R., 2007. Towards a Broad Understanding of the Palm. *Raphia australis*, Unpublished Report, South Africa, Pretoria.
- Maud, R.R., 1980. The climate and Geology of Maputaland. In: Bruton, M., Cooper, K. (Eds.), *Studies on the Ecology of Maputaland*. Cape and Transvaal Printers, Capetown, pp. 1–7.
- Minayeva, T.Y., Sirin, A.A., 2012. Peatland biodiversity and climate change. *Biol. Bull. Rev.* 2 (2), 164–175. <https://doi.org/10.1134/s207908641202003x>.
- Mitsch, W.J., Nahlik, A., Wolksi, P., Bernal, B., Zhang, L., Ramberg, L., 2010. Tropical wetlands: seasonal hydrologic pulsing, carbon sequestration, and methane emissions. *Wetl. Ecol. Manag.* 18, 573–586. <https://doi.org/10.1007/s11273-009-9164-4>.
- Mooney, S.D., Tinner, W., 2011. The analysis of charcoal in peat and organic sediments. *Mires and Peat* 7 (9), 1–18.
- Obando, L.G., Malvassi, L.R., 1993. Geology of Peat Deposits of Costa Rica. *Revista Geologica de América Central* 15, 33–40. <https://doi.org/10.15517/rgc.v015.i13233>.
- Obermeyer, A.A., Strey, R.G., 1969. A New Species of *Raphia* from Northern Zululand and Southern Mozambique. *Bothalia* 10 (1), 29–37. <https://doi.org/10.4102/abc.v10i1.1506>.
- Phillips, S., 1995. *Holocene Evolution of the Changuinola Peat Deposit, Panama: Sedimentology of a Marine-Influenced Tropical Peat Deposit on a Tectonically Active Coast*. PhD Thesis., University of British Columbia, p. 261.
- Phillips, S., Bustin, R.M., 1996. Sedimentology of the Changuinola peat deposit: Organic and clastic sedimentary response to punctuated coastal subsidence. *Geol. Soc. Am. Bull.* 108 (7), 794–814. [https://doi.org/10.1130/0016-7606\(1996\)108<0794:SOTCPD>2.3.CO;2](https://doi.org/10.1130/0016-7606(1996)108<0794:SOTCPD>2.3.CO;2).
- R Core Team, 2020. R: A Language and Environment for Statistical Computing. R Foundation for Statistical Computing. Retrieved from. <https://www.R-project.org/> (accessed 13 January 2022).
- Ramsay, P.J., 1995. 9000 years of sea –level change along the Southern African coastline. *Quat. Int.* 31, 71–75. [https://doi.org/10.1016/1040-6182\(95\)00040-P](https://doi.org/10.1016/1040-6182(95)00040-P).
- Rull, V., Montoya, E., 2014. Mauritia flexuosa palm swamp communities: natural or human-made? A palynological study of the Gran Sabana region (northern South America) within a neotropical context. *Quat. Sci. Rev.* 99, 17–33. <https://doi.org/10.1016/j.quascirev.2014.06.007>.
- Scott, L., 1982. Late Quaternary fossil pollen grains from the Transvaal, South Africa. *Rev. Palaeobot. Palynol.* 36 (1), 241–278. [https://doi.org/10.1016/0034-6667\(82\)90022-7](https://doi.org/10.1016/0034-6667(82)90022-7).
- Sliva, J., Grundling, P.L., Kotze, D., Ellery, F., Moning, C., Grobler, R., Tayler, P.B., 2004. MAPUTALAND – Wise Use Management in Coastal Peatland Swamp Forests in Maputaland, Mozambique / South Africa. In: Wetlands International, Final Project Report (Project No: WGP2 –36 GPI 56).
- Smuts, W.J., 1992. Peatlands of the Natal Mire complex: geomorphology and characterization. *S. Afr. J. Sci.* 88, 474–483. https://hdl.handle.net/10520/AJA0038235_9924.
- South African Weather Service, 2017. A climate Change Reference Atlas. https://www.weathersa.co.za/Documents/Climate/SAWS_CC_REFERENCE_ATLAS_PAGES.pdf (13.09.2024).
- Strachan, K.L., Finch, J.M., Hill, T., Barnett, R.L., 2014. A late Holocene Sea-level curve for the east coast of South Africa. *S. Afr. J. Sci.* 110 (1/2), 1–9. <https://doi.org/10.1590/sajs.2014/20130198>.
- Stuart, B.H., 2004. *Infrared Spectroscopy: Fundamentals and Applications*. John Wiley & Sons, London.
- Succow, M., Jeschke, L., 1986. *Moore in der Landschaft: Entstehung, Haushalt, Lebewelt, Verbreitung Nutzung und Erhaltung der Moore*. Urania Verlag, p. 68 (in German).
- Teickner, H., 2020. Ir: a simple Package to Handle and Preprocess infrared Spectra. <https://github.com/hennigte/ir> (accessed 13 January 2022).
- Teickner, H., Hodgkins, S.B., 2020. Irpeat: Simple Functions to Analyse Mid Infrared Spectra of Peat Samples. Online at. <https://github.com/hennigte/irpeat>.

- Teickner, H., Knorr, K.H., 2022. Improving models to predict holocellulose and Klason lignin contents for peat soil organic matter with mid-infrared spectra. *SOIL* 8, 699–715.
- Toxler, T.G., 2007. Patterns of phosphorus, nitrogen and $\delta^{15}\text{N}$ along a peat development gradient in a coastal mire, Panama. *J. Trop. Ecol.* 23, 683–691. <https://doi.org/10.1017/S0266467407004464>.
- Urquhart, G.R., 1999a. Paleoecological evidence of *Raphia* in the Pre-Columbian Neotropics. *J. Trop. Ecol.* 14, 783–791. <https://doi.org/10.1017/S0266467400010993>.
- Urquhart, G.R., 1999b. Long-term Persistence of *Raphia taedigera* Mart. Swamps in Nicaragua. *Biotropica* 31 (4), 565–569. <https://doi.org/10.1111/j.1744-7429.1999.tb00403.x>.
- van Bellen, S., Larivière, V.J.M., 2020. The ecosystem of peatland research: a bibliometric analysis. *Mires and Peat* 26 (15), 1–30. <https://doi.org/10.19189/MaP.2020.RSC.StA.1977>.
- Von Post, L., 1922. Sveriges geologiska undersöknings torvinventering och några av dess hittills vunna resultat (Geological Survey of Sweden peat inventory and some of its results). *Svenska Mosskulturföréningens Tidskrift* 37, 1–27. <https://pub.epsilon.slu.se/8627/>.
- Von Roeder, M.A.B., 2015. The Impact of Eucalyptus Plantations on the Ecology of Maputaland with Special Reference to Wetlands. Technische Universität München, Master Thesis.
- Walther, S.C., Neumann, F.H., 2011. Sedimentology, isotopes and palynology of late Holocene cores from Lake Sibaya and the Kosi Bay system (KwaZulu-Natal, South Africa). *S. Afr. Geogr. J.* 93 (2), 133–153. <https://doi.org/10.1080/03736245.2011.591982>.
- Wang, M., Moore, T.R., Talbot, J., Riley, J.L., 2015. The stoichiometry of carbon and nutrients in peat formation. *Glob. Biogeochem. Cycles* 29, 113–121. <https://doi.org/10.1002/2014GB005000>.
- Water Research Commission (WRC), 2012. Water Resources of South Africa, 2012 Study. Pretoria, South Africa, Water Research Commission.
- Watmough, S., Gilbert-Parkes, S., Basiliko, N., Lamit, L.J., Lilleskov, E.A., Andersen, R., Zahn, G., 2022. Variation in carbon and nitrogen concentrations among peatland categories at the global scale. *PLoS One* 17 (11), e0275149. <https://doi.org/10.1371/journal.pone.0275149>.
- Woodborne, S., Gandhiwa, P., Hall, G., Patrut, A., Finch, J., 2016. A Regional Stable Carbon Isotope Dendro-Climatology from the South African Summer Rainfall Area. *PLoS One* 11 (7), 1–15. <https://doi.org/10.1371/journal.pone.0159361>.
- Wright, C.I., Lindsay, P., Cooper, J.A.G., 1997. The effect of sedimentary processes on the ecology of the mangrove-fringed Kosi estuary/lake system, South Africa. *Mangrove Salt Marshes* 1, 79–94. <https://doi.org/10.1023/A:1009919816903>.
- Young, D.M., Baird, A.J., Charman, D.J., Evans, C.D., Gallego-Sala, A.V., Gill, P.J., Hughes, P.D.M., Morris, P.J., Swindles, G.T., 2019. Misinterpreting carbon accumulation rates in records from near-surface peat. *Sci. Rep.* 9 (17939), 1–8. <https://doi.org/10.1038/s41598-019-53879-8>.
- Yu, Z., Loisel, J., Brosseau, D.P., Beilman, D.W., Hunt, S.J., 2010. Global peatland dynamics since the Last Glacial Maximum. *Geophys. Res. Lett.* 37, L13402. <https://doi.org/10.1029/2010GL043584>.